

UNCLASSIFIED

AD 410543

DEFENSE DOCUMENTATION CENTER

FOR

SCIENTIFIC AND TECHNICAL INFORMATION

CAMERON STATION, ALEXANDRIA, VIRGINIA



UNCLASSIFIED

NOTICE: When government or other drawings, specifications or other data are used for any purpose other than in connection with a definitely related government procurement operation, the U. S. Government thereby incurs no responsibility, nor any obligation whatsoever; and the fact that the Government may have formulated, furnished, or in any way supplied the said drawings, specifications, or other data is not to be regarded by implication or otherwise as in any manner licensing the holder or any other person or corporation, or conveying any rights or permission to manufacture, use or sell any patented invention that may in any way be related thereto.

N. 63 - 4 - 3

ASD-TDR-63-473

CATALOGED BY DDC  
AS AD No. 410543

ETCH PIT INVESTIGATION OF IRON WHISKERS

TECHNICAL DOCUMENTARY REPORT NO. ASD-TDR-63-473  
April 1963

AF Materials Laboratory  
Aeronautical Systems Division  
Air Force Systems Command  
United States Air Force  
Wright-Patterson Air Force Base, Ohio

Project No. 7353, Task No. 735304

410543

(Prepared under Contract No AF 33(616)-8252  
by The Ohio State University Research Foundation,  
Columbus, Ohio: F. H. Beck and M. G. Fontana,  
authors.)

## NOTICES

When Government drawings, specifications, or other data are used for any purpose other than in connection with a definitely related Government procurement operation, the United States Government thereby incurs no responsibility nor any obligation whatsoever, and the fact that the Government may have formulated, furnished, or in any way supplied the said drawings, specifications, or other data, is not to be regarded by implication or otherwise as in any manner licensing the holder or any other person or corporation, or conveying any rights or permission to manufacture, use, or sell any patented invention that may in any way be related thereto.

The Government has the right to reproduce, use, and distribute this report for governmental purposes in accordance with the contract under which the report was produced. To protect the proprietary interests of the contractor and to avoid jeopardy of its obligations to the Government, the report may not be released for non-governmental use such as might constitute general publication without the express prior consent of The Ohio State University Research Foundation.

Qualified requesters may obtain copies of this report from the ASTIA Document Service Center, Arlington Hall Station, Arlington 12, Virginia. Department of Defense contractors must be established for ASTIA services, or have their "need-to-know" certified by the cognizant military agency of their project or contract.

Copies of this report should not be returned to the Aeronautical Systems Division unless return is required by security considerations, contractual obligations, or notice on a specific document.

## FOREWORD

This report was prepared by The Ohio State University Research Foundation under USAF Contract No. AF 33(616)-8252. The contract was initiated under Project No. 7353, "Characterization of Solid Phase and Interphase Phenomena in Crystalline Structures," and Task No. 735304, "Surface Conditions and Mechanical Response." Work was administered under the direction of the Advanced Metallurgical Studies Branch, Metals and Ceramics Division, Air Force Materials Laboratory, Aeronautical Systems Division, with A2C J. Nilles acting as project engineer.

This report covers work from May 1, 1962 to April 30, 1963.

Technical contributions were made by graduate students, Messrs. C. C. Seastrom and R. M. Shemanski.

## ABSTRACT

The dissolution behavior and the formation of etch-pits in iron whiskers have been studied in the following solutions: 2% nitric acid in alcohol, 4% picric acid in alcohol, a solution of hydrochloric acid in ethanol containing cuprous-chloride, a solution of hydrofluoric acid in water containing ferric-fluoride, copper-ammoniacal chloride solutions both by immersion and electrolytically, and one normal sulfuric acid solution containing 0.2 normal potassium persulfate. Although good etch pits were produced using nital and picral etchants in some cases, the results were not at all satisfactory with respect to reproducibility. The halide-containing etchants usually developed geometric pits, most probably due to the poisoning of dissolution ledges on the iron whisker faces. Etch-pits were produced by copper-ammoniacal-chloride both by immersion in a 2% aqueous solution and electrolytically at 0.004 amp/cm<sup>2</sup> in a 0.5% aqueous solution; however, these pits were usually very small.

Most whiskers were composed of a distinct shell or overgrowth surrounding the core. The shell ranged in thickness from less than one micron up to several microns and this shell thickness appeared to be a critical factor in the development of distinct etch-pits. Etch-pits present in the shell were usually smaller and better defined than in the core.

Dissolution rates were determined using the HF-H<sub>2</sub>O-FeF<sub>3</sub> system and the influence of such variables as crystallographic index of the substrate surface, degree of undersaturation of the dissolving species, and poison concentration were studied. The dissolution rate decreased linearly with increasing poison concentration and decreasing undersaturation. The < 111 > whiskers were found to have a slower rate of dissolution than < 110 > in the HF etchant used.

This technical documentary report has been reviewed and is approved.



W. G. RAMKE  
Actg. Chief, Advanced Metallurgical Studies Branch  
Metals and Ceramics Division  
AF Materials Laboratory

## TABLE OF CONTENTS

<u>Section</u>	<u>Page</u>
I      INTRODUCTION	1
A. Iron Whiskers	1
B. Etch-Pits	1
C. Mechanisms of Dissolution	1
D. Poisons	2
E. Impurities	3
F. Dissolution Rates	4
II     EXPERIMENTAL PROCEDURE	5
III    RESULTS	7
A. Etching by Nitric Acid Solutions	7
B. Etching by Picric Acid Solutions	9
C. Etching by Aqueous Solutions of Copper-Ammoniacal-Chloride	9
D. Etching by Hydrochloric Acid Solutions	23
E. Etching by Hydrofluoric Acid Solutions	29
F. Etching by Sulfuric Acid Solutions	34
IV     DISCUSSION	48
A. Copper-Ammoniacal-Chloride	48
B. Hydrochloric Acid	54
C. Hydrofluoric Acid	55
V      CONCLUSIONS	70
REFERENCES	72
APPENDIX	74

## LIST OF TABLES

<u>Table</u>	<u>Page</u>
1      Compositions of Modified Fry's Reagents	29
2      Description of whiskers shown in Fig. 19 used to study the dissolution rates of aqueous HF solutions poisoned with $\text{FeF}_3$	30
3      Ferric Fluoride Analyses	34
4      Summary of Dissolution Rates	36

# LIST OF FIGURES

<u>Figure</u>		<u>Page</u>
1	Whisker specimens mounted on glass slides using vinyl electrical tape; (top) for immersion etching, and (bottom) for electrolytic etching.	6
2	A hexagonal whisker etched for 60 seconds in 4.0 mole-percent nitric acid solution in ethanol. Rectangular etch-pits can be observed on the {110} face shown. This whisker, from boat No. 504, was 20 $\mu$ in size. X500	8
3	A rectangular whisker from boat No. 542 etched for 20 seconds in 4.0 mole-percent nitric acid solution in ethanol. Very distinct square etch-pits were developed on this {100} face. Whisker size was ~20 $\mu$ . X500	10
4	Rectangular etch-pits formed on hexagonal whiskers by etching for 1-1/2 hours in a 2% aqueous solution of copper-ammoniacal-chloride; (a) etch-pits are aligned at ~55° to the whisker edge; (b) an especially well-developed etch-pit. These whiskers were from boat No. H-92 and were 120 $\mu$ in size.	12
5	A whisker etched for eight hours in a 2% aqueous solution of copper-ammoniacal-chloride; the solution was continually stirred by bubbling air through it. This specimen was a square < 100 > whisker from boat R-1 and was 22 $\mu$ in size. X500	14
6	The effect of a slight deformation on the etching characteristics of an iron whisker; (a) an area well away from the deformation; (b) the localized area where the deformation was applied. Note the etched channel and the slip lines; this whisker was etched in 2% copper-ammoniacal-chloride solution for one hour. The whisker was extracted from boat No. R-1; it was 14 $\mu$ in size and had a < 100 > orientation.	15
7	The apparatus used for electrolytically etching iron whiskers; using a 1.5 volt dry cell, a current of 1.25 $\mu$ a can be realized.	16
8	The schematic circuit diagram for the apparatus used to electrolytically etch iron whiskers	17
9	A {110} whisker face after electrolytically etching for 3 hours in 0.5% copper-ammoniacal-chloride at a current density of ~0.3 amps/cm <sup>2</sup> ; a very large rectangular pit can be seen together with many very small pits. This whisker had < 111 > orientation, was 120 $\mu$ in size, and came from boat No. H-92. X500	19



<u>Figure</u>		<u>Page</u>
10	A hexagonal whisker, 120 $\mu$ in size, etched for 3 hours electrolytically in 0.5% aqueous copper-ammoniacal-chloride at $\sim 0.3$ amp/cm <sup>2</sup> . This specimen was from boat H-92. Many very large, irregular pits can be observed. X500	20
11	This hexagonal whisker was etched for 3 hours electrolytically in 0.5% copper-ammoniacal-chloride at a current density of $\sim 0.3$ amps/cm <sup>2</sup> . Whisker size was 120 $\mu$ and the specimen was extracted from boat No. H-92. Very irregular pits were formed at especially active sites. X500	21
12	Very large rectangular pits formed by electrolytically etching in 0.5% aqueous copper-ammoniacal-chloride solution for 3 hours at $\sim 0.3$ amps/cm <sup>2</sup> ; (a) focusing at the bottom of the pit shows the truncated-pyramidal shape of the pit; (b) focusing on the {110} face of the whisker. Whisker size was 120 $\mu$ and the orientation was $\langle 111 \rangle$ . This whisker came from boat No. H-92.	22
13	A hexagonal whisker etched for 20 seconds in a modified Fry's reagent containing 0.03 gm CuCl <sub>2</sub> . Some rectangular pits can be observed, but on the whole, the etch-pits were not well-contained. This whisker was from boat No. 504 and was 15 $\mu$ in size. X500	24
14	This whisker, from boat No. R-1, was etched for 5 seconds in Fry's reagent containing 0.01 gm CuCl <sub>2</sub> . The whisker shape was hexagonal and many distinct, rectangular etch-pits can be observed on the {110} face shown. The size of this whisker was 35 $\mu$ . X500	26
15	Rectangular etch-pits, aligned along a tilt boundary, were developed on this {110} face of a $\langle 111 \rangle$ whisker by immersion in a Fry's reagent containing 0.01 gm CuCl <sub>2</sub> for 10 seconds. This whisker was 30 $\mu$ in size and came from boat R-1. X500	27
16	This {110} face of a $\langle 111 \rangle$ whisker, 30 $\mu$ in size, shows distinct rectangular etch-pits. These pits were formed by immersion for 10 seconds in a Fry's reagent containing 0.001 gm of CuCl <sub>2</sub> . This whisker was extracted from boat No. 504. X500	28
17	Dissolution rate of iron whiskers of various growth orientations as a function of HF conc. in water.	31
18	Dissolution at dislocation sites along a tilt-boundary produced by etching in 9.0 mole-percent HF acid solution in water for 15 seconds; the dissolution rate was 1.6 $\mu$ /minute. This whisker was 80 $\mu$ in size, square, and extracted from boat No. H-93. Some very small, square etch-pits are still visible. X500	32

<u>Figure</u>		<u>Page</u>
19	Dissolution rate of iron whiskers of various growth orientations etched in 3.0 mole-percent HF solution in water as a function of the conc. of $\text{FeF}_3$ hydrate ( $\text{Fe} = 31.21\%$ ) poison used.	33
20	A rectangular whisker etched in 3.0 mole-percent HF in water and containing $6.5 \times 10^{-7}$ mole-fraction of $\text{FeF}_3$ . The immersion time was 60 seconds and the whisker was taken from boat No. 539; the size was $40\mu$ . Dissolution ledges are quite distinct on {100} face shown here. The dissolution rate was $2.5\mu/\text{minute}$ . X500	35
21	Etch pits at as-grown and deformation dislocations. Rectangular whisker, (100) face, from boat H-121. a) Etched for 1-1/2 min in 1N $\text{H}_2\text{SO}_4 + 0.2\text{N K}_2\text{S}_2\text{O}_8$ . 1000X b) Deformed after the 1-1/2 min etch, then etched for 1 additional minute. 1000X	38
22	Removal of whisker shell. Rectangular whisker, (100) face, from boat H-121. a) Etched for 1-1/2 min in 1N $\text{H}_2\text{SO}_4 + 0.2\text{N K}_2\text{S}_2\text{O}_8$ . 1000X b) Same as (a) except etched for 2-1/2 min.	39
23	Etching of whisker shell. Square whisker, from boat 529. Etched for 2 min in 1N $\text{H}_2\text{SO}_4 + 0.2\text{N K}_2\text{S}_2\text{O}_8$ . 1000X	40
24	Etch pits at as-grown dislocations. Square whisker, from boat 538. Etched 1-1/2 min in 1N $\text{H}_2\text{SO}_4 + 0.2\text{N K}_2\text{S}_2\text{O}_8$ . 1000X	41
25	Etching of whisker shell. Hexagonal whisker, from boat H-89. Etched for 1/2 min in 1N $\text{H}_2\text{SO}_4 + 0.2\text{N K}_2\text{S}_2\text{O}_8$ . 1000X	41
26	Etched pits at as-grown and deformation dislocations in whisker core. Plate-like whisker, (100) face, from boat H-75. a) Etched for 9 min in 1N $\text{H}_2\text{SO}_4 + 0.2\text{N K}_2\text{S}_2\text{O}_8$ . 1000X b) Deformed after etching for 9 min, then etched for 8 min following deformation. 1000X	43
27	Removal of whisker shell. Rectangular whisker, (100) face, from boat H-121. a) Etched for 1 min in 1N $\text{H}_2\text{SO}_4 + 0.2\text{N K}_2\text{S}_2\text{O}_8$ . 1000X b) Same as (a) except etched for 6-1/2 min. c) Deformed after etching 6-1/2 min and then etched for an additional 5 min. 1000X	44
28	Etching of the core of a deformed whisker. Hexagonal whisker from boat H-89. a) Deformed after etching 4 min in 1N $\text{H}_2\text{SO}_4 + 0.2\text{N K}_2\text{S}_2\text{O}_8$ and then re-etched for 10 min following deformation. 1000X b) Same as (a) except for 16 min following deformation.	45

<u>Figure</u>		<u>Page</u>
29	Removal of whisker shell. Hexagonal whisker, from boat H-91. a) Etched for 5 min in 4% picral. 1000X b) Etched for 45 min in 4% picral. 1000X c) Etched for 45 min in 4% picral followed by 1-1/2 min etch in 1N H <sub>2</sub> SO <sub>4</sub> + 0.2N K <sub>2</sub> S <sub>2</sub> O <sub>8</sub> . 1000X	46
30	Removal of whisker shell. Hexagonal whisker, from boat H-91. a) Etched for 4 min in 2% nital. 1000X b) Same as (a) except etched for 10 min. c) Etched as stated in (b) followed by 1/2 min etch in 1N H <sub>2</sub> SO <sub>4</sub> + 0.2N K <sub>2</sub> S <sub>2</sub> O <sub>8</sub> . 1000X	47
31	Removal of whisker shell. Hexagonal whisker, from boat H-91. a) Etched for 4 min in 4% picral. 1000X b) Etched for 45 min in 4% picral, and then 5 min in 1N H <sub>2</sub> SO <sub>4</sub> + 0.2N K <sub>2</sub> S <sub>2</sub> O <sub>8</sub> . 1000X c) Etched as stated in (b) followed by a 4 min etch in 4% picral. 1000X d) Etched as stated in (c) followed by a 3 min etch in 2% nital. 1000X	49
32	Rotation of shell and core. Rectangular whisker, (100), face from boat H-121. Etched for 4-1/2 min in 1N H <sub>2</sub> SO <sub>4</sub> + 0.2N K <sub>2</sub> S <sub>2</sub> O <sub>8</sub> . 1000X	50
33	The principal unit triangle of a [100] stereographic projection showing the slip systems operative in each area.	52
34	(a) The intercepts of a {112} and a {123} with a {100} type plane. (b) Probable slip plane operating in a <100> iron whisker. (c) Dislocation loops on a (112)[111] slip system showing a pile-up at the corner.	53
35	The amount of FeF <sub>3</sub> · 3H <sub>2</sub> O as a function of mole-percent of HF in 100 gms saturated solution in H <sub>2</sub> O at 25°C at equilibrium in the HF - FeF <sub>3</sub> -H <sub>2</sub> O system.	56
36	Influence of an oxidizing agent on the polarization curves for the corrosion of iron in acids.	62
37	Polarization behavior of iron in 1N H <sub>2</sub> SO <sub>4</sub> + 0. 0.2N K <sub>2</sub> S <sub>2</sub> O <sub>8</sub> .	63
38	Polarization behavior of iron in 1N H <sub>2</sub> SO <sub>4</sub> + 0. 5N (NH <sub>4</sub> ) <sub>2</sub> S <sub>2</sub> O <sub>8</sub> .	64
39	Schematic Representation of Etch Pits as Projected on (100) and (110) faces, a through e are (100) projections.	65

<u>Figure</u>		<u>Page</u>
40	(a) Regions of a unit triangle within which the indicated resolved shear stresses in a bcc lattice is higher than other resolved shear stresses. (b) Intersection of slip plane $(\bar{2}11)$ with whisker faces $(0\bar{1}1)$ and $(01\bar{1})$	67
41	Traces of slip systems on whisker faces	68
42	Potential time traces in $1N H_2SO_4 + 0.2N K_2S_2O_8$ , a) Rectangular whisker, b) Square whisker. The initial instability in (b) resulted from a loose connection in the measuring circuit. 30, 40, 50 correspond to -300, -400, -500 millivolts active to the saturated calomel electrode (SCE).	69

## I. INTRODUCTION

### A. IRON WHISKERS

Iron whiskers are filamentary single crystals which are believed to be nearly perfect crystallographically, at least those of sub-micron size. The characteristic morphologies of whiskers have been studied by many investigators<sup>1-4</sup> who concluded that ideally three axial growth directions predominate, viz,  $\langle 100 \rangle$ ,  $\langle 110 \rangle$ , or  $\langle 111 \rangle$ , having square, rectangular, or hexagonal cross sections, respectively. The  $\langle 100 \rangle$  -type whisker is bounded by four  $\{100\}$  planes; the  $\langle 110 \rangle$  -type has two  $\{100\}$  faces and two  $\{110\}$  faces, the  $\{100\}$  faces being wider and generally more perfect; the  $\langle 111 \rangle$  -type is bounded by six  $\{110\}$  planes; however, Rambauski and Gruenzel<sup>5</sup> have reported that hexagonal whiskers may be bound by  $\{211\}$  planes.

### B. ETCH-PITS

Etch-pit techniques represent a relatively simple method of studying defect structures in single crystals. Crystallographic orientations may also be determined from well-defined geometrical etch-pits due to the crystalline symmetry of the substrate surface which is demonstrated in the pit shape. In order that these techniques be applicable, an etchant that develops pits at dislocation sites with a minimum amount of background dissolution and having regular, geometrical shapes delineated by low index planes is required. Coleman<sup>12</sup> observed dislocation etch-pits on iron whiskers etched in nital and picral. He reported that it was difficult to produce pits at as-grown dislocation sites and that plastic deformation was required to obtain distinct etch-pits on  $\{100\}$  faces.

Several investigators have reported the formation of etch-pits on larger iron crystals. Liss<sup>7</sup> and Boswell<sup>8</sup> prepared iron surfaces by electropolishing in chromic-acetic acid, followed by successive etching in 1% nital for one minute and in 0.5% picral for five minutes. Smith and Mehl<sup>9</sup> formed etch-pits on  $\{110\}$  planes using aqueous solutions of copper-ammoniacal-chloride both by immersion and by electrolytic etching. Svetchnikoff<sup>10</sup> reported that  $\{100\}$ ,  $\{111\}$ , and  $\{110\}$  planes were developed by aqueous copper-ammoniacal-chloride solutions. Gorsuch<sup>6</sup> used a solution of HCl in ethanol containing cupric-chloride to reveal dislocations in iron whiskers, but these were restricted to dislocations decorated with carbon.

### C. MECHANISMS OF DISSOLUTION

Probable mechanisms for dissolution have been presented by Young<sup>11</sup> and also by Mendelson.<sup>13</sup> As discussed by Young, dissolution occurs in steps. An atomic ledge or step must first be nucleated on the surface; subsequently, the monatomic ledge can propagate across the surface as atoms go into solution. The second step most probably involves a complex process, including the oxidation of the metal along the ledge and the subsequent dissolution of the metallic oxide.

---

Manuscript released April 1963 by the authors for publication as an ASD Technical Documentary Report.

Atomic ledges are inherent characteristics of non-close-packed planes; however, for close-packed planes, monatomic ledges must be nucleated and, in many cases, this is, in fact, the rate-controlling step in the dissolution kinetics. Cabrera<sup>13</sup> reported that dislocations are probable sites for ledge nucleation, and he showed that dislocations are, indeed, regions of undersaturation with respect to the remainder of the lattice. The nucleation of ledges at dislocations is favored because of the contribution of the strain energy associated with the lattice misfit. Cabrera concluded that (a) nucleation of atomic steps is energetically favored at dislocation sites; (b) the nucleation of many monatomic ledges in one relatively constrained area results in the formation of an etch-pit; and (c) the formation of an etch-pit depends upon the dissolution kinetics, viz, the relative rates of ledge nucleation and step propagation. The rate of ledge propagation must be less than the rate of nucleation in order for pits to develop. Since nucleation of monatomic steps is usually the rate-controlling step on close-packed faces in metallic crystals, the ledge propagation must be retarded. Therefore, the etchant should contain a "poison" which can effectively bring about this retardation.

#### D. POISONS

Frank<sup>14</sup> has developed a theory of dissolution modified in such a way as to include the effect of poisons. The poison is assumed to adsorb strongly on the surface but, because of its low concentration, requires time to reach adsorption equilibrium. Wide ledges have a greater concentration of adsorbate than narrow ledges and, hence, the motion of the wider ledges is more greatly suppressed. An initially flat, low-index surface can be thought of as a very wide ledge and has a large concentration of adsorbed poison. Since the velocity of the leading ledge will determine the rate of change of pit width, the principal effect of a poison on low-index faces is to slow down the leading ledges of a pit and cause a pile-up of subsequently formed ledges. In this way a distinct pit of finite depth is developed.

Young<sup>11</sup> showed that it was necessary to add bromide ions in order to develop pits on the {111} faces of copper crystals and that chloride ions were required for pit formation on {100} faces. Lovell and Wernick<sup>15</sup> and Livingston<sup>16</sup> used  $\text{FeCl}_3$ ,  $\text{HCl}$ ,  $\text{HAc}$ , and  $\text{Br}_2$  solutions to produce pits on {111} faces of copper. Dislocation etch-pits on the basal plane of zinc crystals were produced by Rosenbaum and Saffren<sup>17</sup> using halide acids, viz,  $\text{HCl}$ ,  $\text{HBr}$ , and  $\text{HI}$ , dissolved in various solutions. Gilman, Johnston, and Sears<sup>18</sup> explained the formation of dislocation etch-pits in  $\text{LiF}$  using  $\text{FeF}_3$  in solution such that  $\text{Fe}^{+++}$  ions served as a poison. Mendelson<sup>12</sup> used  $\text{FeCl}_3$  dissolved in glacial acetic acid in order to develop etch pits in sodium chloride crystals. Gorsuch<sup>6</sup> used  $\text{Cl}^-$  ions to produce etch pits at decorated dislocation sites in iron whiskers.

The above reports in the literature show that etch pits at dislocation sites have been produced in a variety of materials, including fcc, bcc, hcp, and ionic crystals, using etchants containing suitable poisons to retard lateral step propagation. The poison is usually thought to be in solution but Berlec<sup>19</sup> suggested that impurities in the crystal could serve as poisons.

The optimum poison concentration varies for each system and with the imposed conditions, i.e., temperature, etc., but the amount of poison required is usually low. A concentration of  $2 \times 10^{-8}$  mole-fraction  $\text{FeF}_3$  was found to suffice for etch-pit formation in  $\text{LiF}$ .<sup>18</sup>

From these results, it can be concluded that an etchant suitable for developing dislocation sites should include two components, each with a specific purpose: (a) an oxidizing agent and (b) a species to serve as a poison. Halide ions and halogen molecules appear to retard ledge dissolution most universally as was reported above and in additional papers.<sup>20-27</sup>

#### E. IMPURITIES

The presence of a small amount of impurity in a crystal is sufficient to produce a Cottrell atmosphere around a dislocation. The presence of the impurity atmosphere around the dislocation results in these dislocations being referred to as "dirty" dislocations, as contrasted to "clean," newly-formed dislocations. All old, or grown-in, dislocations will be "dirty" since even the very smallest impurity concentrations in the growth atmosphere would suffice to contaminate all dislocation sites. All "clean" dislocations, due to deformation, etc., will have broken away from impurity atmospheres upon movement due to the applied stresses. A reliable dislocation etchant should be able to distinguish between "clean" and "dirty" dislocations as well as "edge" and "screw" dislocations by means of the size and shape of the etch pits.

The presence of impurity atmospheres around a dislocation may lead to a chemical driving force for pit-formation at the dislocation site. When a chemical rather than a physical motivation due to strain energy is present, the pits are apt to be conical rather than geometrical in shape since the etchant would preferentially attack the impurity. Young<sup>11</sup> summarized the criteria for etch-pit formation at dislocation sites as follows:

##### 1. For clean dislocations:

- (a) Pits can be developed at dislocation-surface intersections only on close-packed crystalline faces.
- (b) In order for pits to be readily observable, it is necessary to include a "poison" in the etchant to retard ledge dissolution.
- (c) Such pits would have crystallographic shapes.
- (d) Using suitable reagents, a difference in appearance (size) of pits formed at edge or screw sites might be expected.
- (e) Pits at clean dislocations may differ in appearance (size) from pits at dislocation having an impurity atmosphere.

c. For dirty dislocations:

(a) The impurity atmosphere may cause the region around the dislocation to be chemically more active, thus promoting step nucleation at such points. Therefore, it would be possible to form pits only at dirty dislocations, yet only on close-packed faces.

(b) If the impurity is at such a concentration that segregation can occur at dislocations, the dislocation acts as a live source of impurity atoms. For suitable etchants, pits would be formed at such dislocations on all crystal faces, and the resulting pits would be, in fact, conical in shape.

The models discussed by Young for etch-pit formation, i.e., the agglomeration of atomic ledges to form multi-atomic terraces bounded by certain crystallographic surfaces, also have been discussed by Cabrera and Vermilyea<sup>28</sup> and Frank.<sup>14</sup>

F. DISSOLUTION RATES

A consequence of the above theory of dissolution<sup>14</sup> is that concave surfaces should be bound in the limit by slowly dissolving planes. This was verified for the dissolution of germanium.<sup>29</sup> A 1-cm diameter hemispherical hole was ground on a {100} face. After etching in a solution composed of  $H_2O_2$ , HF, and  $H_2O$ , the hollow was found to be bound by {111} and {100} planes. Independent measurements of dissolution rates indicated that the {111} and {100} planes dissolved at a lower rate than other orientations.

Engell<sup>30</sup> found that the shape of the pits on alpha iron single crystals depended on the rate of dissolution of the face. When the rate of dissolution was high, as represented by the solution  $1N H_2SO_4 + 0.5N (NH_4)_2S_2O_8$ , the {111} plane of a {111}-{100} galvanic cell dissolved at a faster rate than the {100} plane. Other orientations were assumed to have a dissolution rate between {111} and {100}. The {111} plane dissolved only slightly faster than the {100} when the over-all rate of dissolution was reduced, as represented by the solution  $1N H_2SO_4 + 0.02N K_2S_2O_8$ . No difference in dissolution rate was noted in  $1N H_2SO_4$ , which represents the lowest dissolution rate. The measurement of dissolution rate was made by dissolving such a small amount of iron that there was very little change in the appearance of the surface.

If the iron samples were allowed to dissolve for a considerably longer time, pits bound by five {100} faces were formed on a {100} plane in  $1N H_2SO_4$ . At the high dissolution rate represented by the solution  $1N H_2SO_4 + 0.5N (NH_4)_2S_2O_8$ , the pits on a {100} plane were bound by four {111} faces, while triangular pits bound by three {100} faces were formed on a {111} surface. In the  $1N H_2SO_4 + 0.02N K_2S_2O_8$  solution, transition pits which appeared to be bound by four {111} side faces and a {100} bottom were formed on a {100} surface.



The occurrence of pits bound by {100} faces agrees with the theory that concave shapes should be bound by the more slowly dissolving planes. The pits bound by {111} faces do not agree directly with the theory. However, Engell showed that the {111} faces are very likely composed of small steps bound by planes other than {111}. If these other planes were low dissolution rate planes, then Engell's observations would still be consistent with the theory.

To summarize the theory of dissolution as it pertains to etch pit formation, the requirements for the formation of a well-defined etch pit are: (a) a low-index face containing a low density of ledges; (b) selective ledge sources, most likely at dislocation sites; and (c) the presence of an impurity poison to retard ledge motion.

## II. EXPERIMENTAL PROCEDURE

The iron whiskers used in this study were grown by means of hydrogen reduction of ferrous chloride by the Advanced Metallurgical Studies Branch, Metals and Ceramics Division, Air Force Materials Laboratory, Wright-Patterson Air Force Base, Ohio.

The whiskers were mounted in various ways depending upon the type of experiment to be conducted and the observations to be made. For complete examination of all faces, the whiskers were glued into the ends of small glass capillary tubes and these capillary tubes in turn were mounted on an apparatus which could rotate the whisker  $360^\circ$  around its growth axis. In this way, corrosive attack in a given environment could be studied on each whisker face. For those experiments in which changes on a single whisker face were observed, the whiskers were mounted in a fixed position on glass slides by means of vinyl electrical tape. Using this technique, observations of the same surface area were assured and changes in the surface morphology, especially the edges, could be easily followed.

For electrolytic measurements, the same methods of mounting were employed, with slight modifications. In order to measure the single electrode potential of a corroding whisker, an electrical connection must be made with the whisker. This connection must be insulated from the environment. For those whiskers mounted on glass slides, a 5 mil platinum wire was taped to the glass slide and fastened to one end of the whisker by means of silver print, a silver paint used in electrical printed circuits. The entire mount was then covered with epoxy resin and subsequently Glyptal red enamel. Figure 1 shows whiskers mounted on glass slides for immersion etching (top) and for electrolytic experimentation (bottom). In those cases requiring complete surface examination of the corroded whisker, the specimen was fastened into the end of a "hypodermic" needle by means of "dag," dispersion No. 154, a colloidal graphite dispersion in alcohol, manufactured by the Acheson Colloids Co. of Port Huron, Michigan. The needle was insulated from the environment by coating it with clear "finger-nail" polish. Mounted in this way, the whisker could be rotated under the microscope for complete examination.

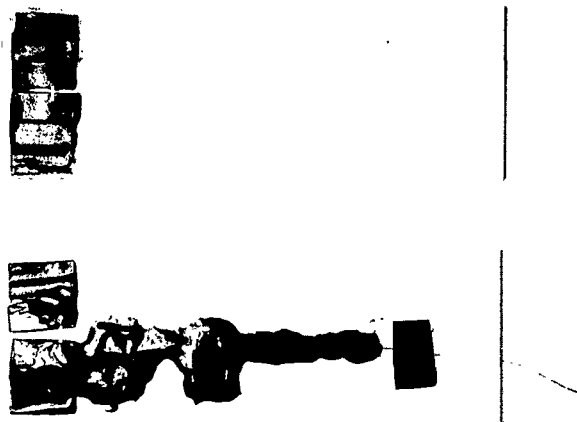


Figure 1. Whisker specimens mounted on glass slides using vinyl electrical tape; (top) for immersion etching, and (bottom) for electrolytic etching.

The environments used in this study were:

- (1) 2% by volume of concentrated nitric acid in ethyl alcohol (nital);
- (2) 4% solution by weight of picric acid in methyl alcohol (picral);
- (3) aqueous copper-ammoniacal-chloride solutions
  - (i) a 2% solution for immersion tests
  - (ii) a 0.5% solution for electrolytic etching;
- (4) 8 ml concentrated hydrochloric acid in 100 ml ethyl alcohol containing cupric-chloride (.001 gm to 0.5 gm), ferrous-chloride (0 to 0.2 gm), and saturated with picric acid;
- (5) solutions of varying amounts of concentrated hydrofluoric acid in water (up to 25 mole-percent);
- (6) 3.0 mole-percent concentrated hydrofluoric acid in water containing ferric-fluoride (0 to  $6.5 \times 10^{-8}$  mole-fraction);
- (7) one normal sulfuric acid solution in water containing 0.2N  $K_2S_2O_8$ .

The technique employed for all the above media was to immerse the appropriately mounted whisker in the etchant for a given amount of time. The solution was maintained at room temperature and constantly stirred by means of a magnetic stirrer. After removal from the etchant, the whiskers were thoroughly rinsed in distilled water and dried in a blast of hot air. Finally, the whiskers were examined under the microscope and photographed when the results were satisfactory for recording.

### III. RESULTS

#### A. ETCHING BY NITRIC ACID SOLUTIONS

Although pits were produced using nital as an etchant, it was found that the results were much less consistent or reproducible as compared to other etchants. Therefore, the role of nital in these studies was restricted to a complementary service, viz., comparison with tests conducted in the more satisfactory environments. Figure 2 shows rectangular etch-pits formed on a {110} face of a  $\langle 111 \rangle$  oriented whisker etched for 60 seconds in a 4.0 mole-percent  $HNO_3$  in ethanol solution. These geometrical pits are largely masked

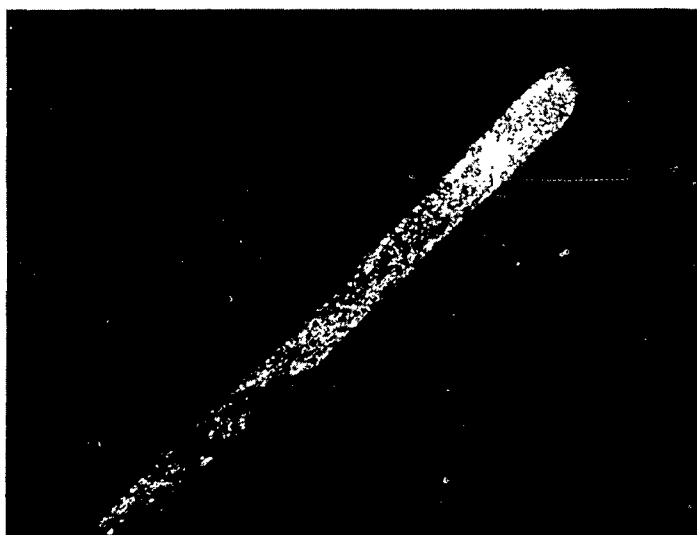


Figure 2. A hexagonal whisker etched for 60 seconds in 4.0 mole-percent nitric acid solution in ethanol. Rectangular etch-pits can be observed on the  $\{110\}$  face shown. This whisker, from boat No. 504, was 20 $\mu$  in size.

X500

by the nondescript attack occurring over most of the whisker face. Figure 3 shows distinct square etch-pits on a {100} face of a rectangular  $\langle 110 \rangle$  oriented whisker etched for 60 seconds in a 4.0 mole-percent  $\text{HNO}_3$  solution in ethanol. The whiskers in these two figures are of comparable size, i.e., approximately 20 $\mu$ . These results show that nital develops better pits on {110} faces than on {100} faces. However, the growth conditions should be noted and the effects of any variations in these conditions ascertained before any confidence can be placed in the above trends. The hexagonal whisker in Fig. 2 was extracted from boat 504. These whiskers were grown from commercial  $\text{FeCl}_2 \cdot 4\text{H}_2\text{O}$  which was heated in an argon atmosphere to 710°C, reduced by hydrogen at 710°C for two hours, and then furnace cooled in hydrogen. The rectangular whisker in Fig. 3 was taken from boat 542 which again used commercial  $\text{FeCl}_2 \cdot 4\text{H}_2\text{O}$  but which was heated to 660°C in a helium atmosphere. At this temperature, the hydrogen flow was initiated and the temperature subsequently raised to 710°C and held there for three hours. These whiskers were finally furnace cooled in a hydrogen atmosphere.

The above results are representative of the tests in which good etch-pits were developed; however, many more tests were conducted using nital which showed only general, uniform attack. The positive results were significant enough to warrant the use of nital in a complementary manner, relative to more reliable etchants.

#### B. ETCHING BY PICRIC ACID SOLUTIONS

This etchant also lacked the required reproducibility and consistency of results to be satisfactory for extensive testing. In some cases, hexagonal whiskers etched in 4% picral contained rectangular etch-pits delineated by two {100} planes. These pits were relatively shallow and after extended etching, considerable background attack obliterated the geometrical etch-pits formed initially. Similarly to nital, picral tended to develop etch-pits better on the {110} faces. Again, this etchant proved useful only for supplementary experimentation.

#### C. ETCHING BY AQUEOUS SOLUTIONS OF COPPER-AMMONIACAL-CHLORIDE

An acidic solution of cuprous chloride was prepared by the Winkler method:<sup>31</sup>

"Added a mixture of 86 gm of  $\text{CuO}$  and 17 gm of finely divided metallic  $\text{Cu}$ , made by reduction of  $\text{CuO}$  with  $\text{H}_2$ , to a solution of  $\text{HCl}$  made by diluting 650 ml of conc.  $\text{HCl}$  with 325 ml of  $\text{H}_2\text{O}$ . After the mixture had been added slowly and with frequent stirrings, a spiral of copper wire was suspended in the bottle, reaching all the way to the bottom. After occasionally shaking, the solution was ready for use when it became colorless."



Figure 3. A rectangular whisker from boat No. 542 etched for 20 seconds in 4.0 mole-percent nitric acid solution in ethanol. Very distinct square etch-pits were developed on this {100} face. Whisker size was  $\sim 20\mu$ .

X500

This acidic solution was then neutralized with ammonium hydroxide until an ammonia odor persisted, the excess of metallic copper being kept in solution. The procedure was:<sup>31</sup>

"800 ml of acidic cuprous chloride, prepared by the Winkler method, was poured into four liters of  $H_2O$ . The precipitate was transferred to a 250 ml graduate; after several hours, the liquid above the 50 ml mark was siphoned off and the graduate refilled with 7.5%  $NH_4OH$  solution which was prepared by diluting 50 ml of conc.  $NH_4OH$  with 150 ml  $H_2O$ . The solution was then shaken well and allowed to stand for several hours."

#### 1. Etching by Immersion

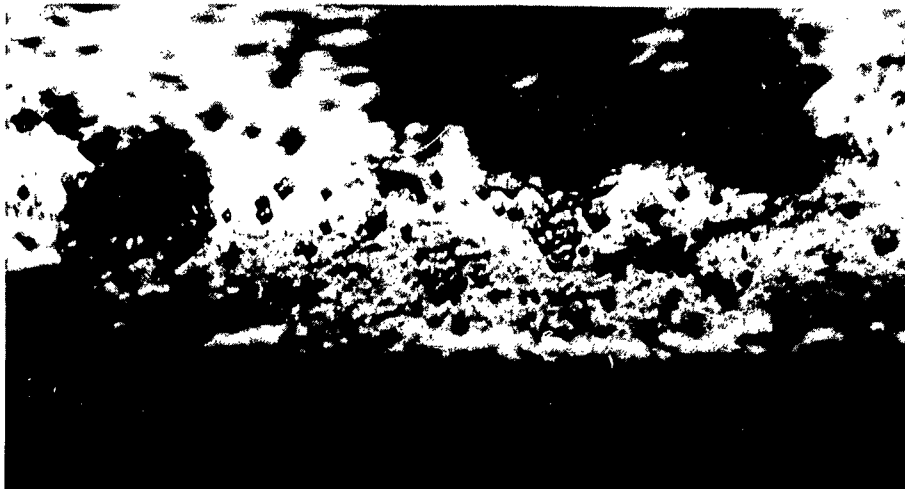
The whiskers used for etching by immersion tests were from boats No. H-92 and No. R-1. There was an approximately equal number of < 111 >, hexagonal, and < 100 >, square, whiskers; no < 110 >, rectangular, whiskers were used for these tests. The whiskers were on the average 50 $\mu$  in diameter with a range from 14 $\mu$   $\longrightarrow$  120 $\mu$ . All specimens used had bright faces with usually good shape; however, deformed ends and slight longitudinal twisting or kinking was not uncommon.

A 2% copper-ammoniacal-chloride in water solution was used for all the tests.<sup>10</sup> Since the solution contained a finely dispersed white precipitate which would turn dark after standing 24 hours or more, the aqueous solutions were made fresh each time, using the same stock solution. Tests were run using a stagnant solution and solutions continuously stirred by bubbling air through the solution for times up to eight hours.

Pits of seemingly rectangular shape were developed in stagnant solutions, (Fig. 4). These pits were extremely small and appeared to form within 3-5 minutes. The pit size increased only very slightly for periods of immersion up to eight hours. These pits appeared to be aligned with respect to the edges of the lateral faces and seemed to form in clusters. Neither the pit density nor the pit size increased appreciably with time.

Competing with the formation of etch-pits was the plating-out of copper upon the whisker faces, (dark areas of Figure 4). This began immediately upon immersion and after eight hours the whiskers were approximately 99% covered with copper. This copper-plate was very "spongy" but yet attempts to remove it without damage to the whiskers were futile. One whisker was etched in 0.5% ammonium persulfate solution in order to remove the copper which plated out.<sup>32</sup> However, the copper remained and the whisker was strongly attacked, leaving a very irregular surface.

The effect of stirring the etchant was demonstrated by slowly bubbling air through the solution throughout the immersion period. Pits were formed which were not unlike the pits formed in stagnant solutions except that they seemed less geometric in shape. The pit size was slightly larger and the pit density approximately the same. For periods up to eight



(a) 1000X



(b) 1000X

Figure 4. Rectangular etch-pits formed on hexagonal whiskers by etching for 1-1/2 hours in a 2% aqueous solution of copper-ammoniacal-chloride; (a) etch-pits are aligned at  $\sim 55^\circ$  to the whisker edge; (b) an especially well-developed etch-pit. These whiskers were from boat No. H-92 and were  $120\mu$  in size.



hours, the faces were heavily covered with "spongy" copper but the areas free from copper showed very little effect of the eight-hour immersion (Fig. 5). This was contrary to the whiskers etched for eight hours in a stagnant solution which showed heavily faceted areas. The pit size and the pit density were slightly better in the stirred solutions; however, the pit shape was frequently irregular.

In order to test the reliability of aqueous solutions of copper-ammoniacal-chloride for development of etch pits at dislocation sites, a whisker was slightly deformed by bending before immersion in the etchant. After one hour in 2% copper-ammoniacal-chloride, evidence of the deformation was clearly visible; etch pits were formed along traces of slip planes as would be expected if pits were developed at dislocations sites (Fig. 6). The pits most probably corresponded to fresh, clean dislocations and the shapes of the pits observed were of no regular geometry. However, this showed, if only qualitatively, that dislocation sites were developed by this etchant, and that the results observed can be expected to represent, at least partially, the defect structure. There is no reason at this time to expect that all of the dislocation sites were developed.

## 2. Electrolytic Etching

Copper-ammoniacal-chloride used electrolytically as an etchant was suggested by Smith and Mehl<sup>9</sup> and also by Kehl.<sup>33</sup> Due to the very small surface area of the whiskers, an apparatus was constructed to provide a very low current density, 0.5 amps/dm<sup>2</sup>. The apparatus used is shown in Fig. 7 and its schematic wiring diagram is illustrated in Fig. 8. Using a 1.5-volt dry cell, a range of current from 1.25  $\mu$ a  $\longrightarrow$  5 ma d.c. was possible. A platinum cathode was used in all cases. All electrical connections to the actual whiskers were made by means of "dag." Therefore, it was necessary to ascertain the resistance of a typical "dag" connection in order to determine the current used. Three whiskers mounted on glass slides by means of vinyl electrical tape were tested, electrical connections being made by gluing "sewing" needles to the whisker ends. The resistance of the "dag" mounting was quite negligible,  $\approx$  500  $\Omega$ , compared to a circuit resistance normally used of approximately 1,000,000  $\Omega$ . The "dag" resistance was, therefore, ignored in all further work.

For the electrolytic work, two hexagonal whiskers were chosen from boat H-92 and mounted at the ends of "hypodermic" needles by means of "dag". These whiskers will be designated (1) and (2) for all further discussion.

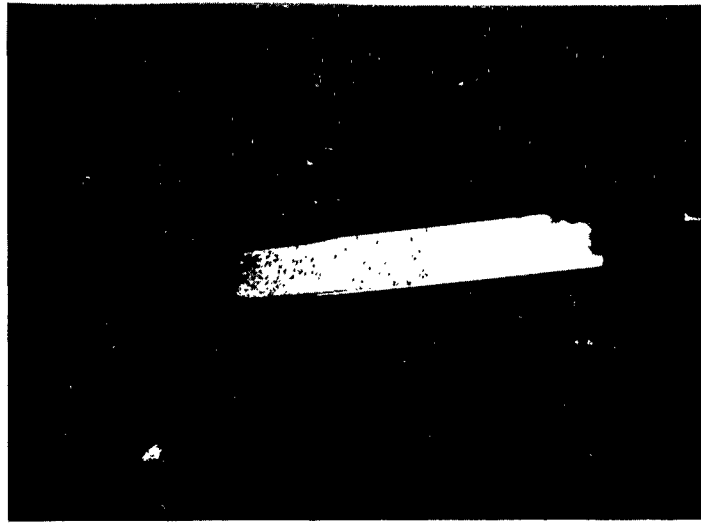
### Whisker Number 1

This whisker was a hexagonal whisker of approximately 120 $\mu$  in diameter and about 0.3 cm in length. The lateral faces were relatively good, but prominent tilt boundaries were visible. The approximate surface area was  $1.26 \times 10^{-2}$  cm<sup>2</sup>.



Figure 5. A whisker etched for eight hours in a 2% aqueous solution of copper-ammoniacal-chloride; the solution was continually stirred by bubbling air through it. This specimen was a square  $\langle 100 \rangle$  whisker from boat R-1 and was  $22\mu$  in size.

X500

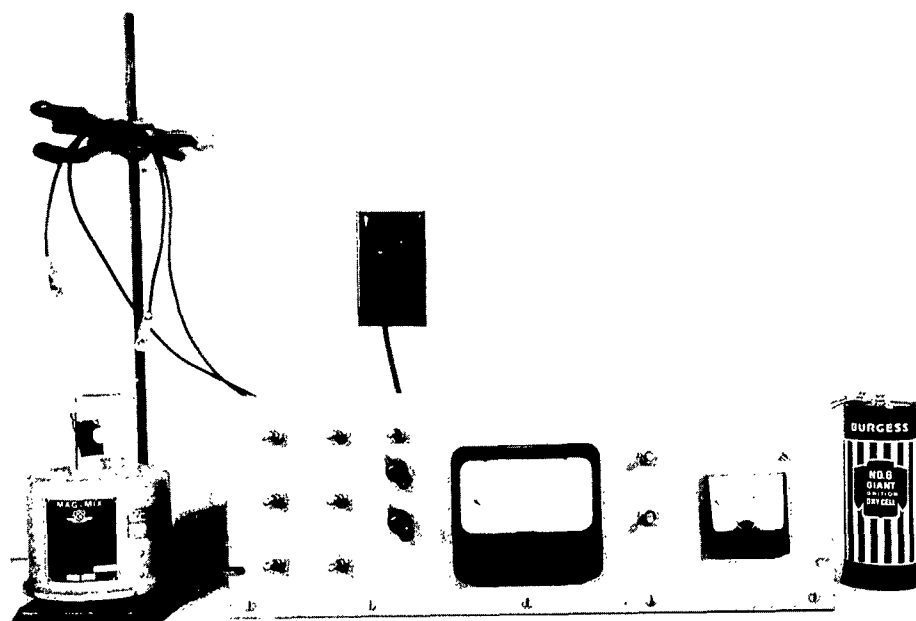


(a) 500X

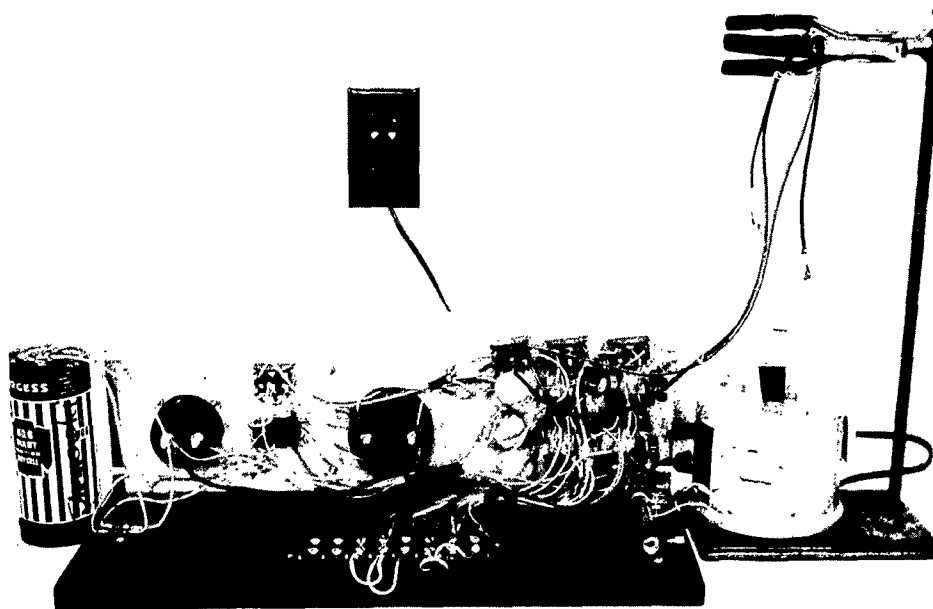


(b) 500X

Figure 6. The effect of a slight deformation on the etching characteristics of an iron whisker; (a) an area well away from the deformation; (b) the localized area where the deformation was applied. Note the etched channel and the slip lines; this whisker was etched in 2% copper-ammoniacal-chloride solution for one hour. The whisker was extracted from boat No. R-1; it was  $14\mu$  in size and had a  $\langle 100 \rangle$  orientation.



(a)



(b)

Figure 7. The apparatus used for electrolytically etching iron whiskers; using a 1.5 volt dry cell, a current of  $1.25\mu\text{A}$  can be realized.

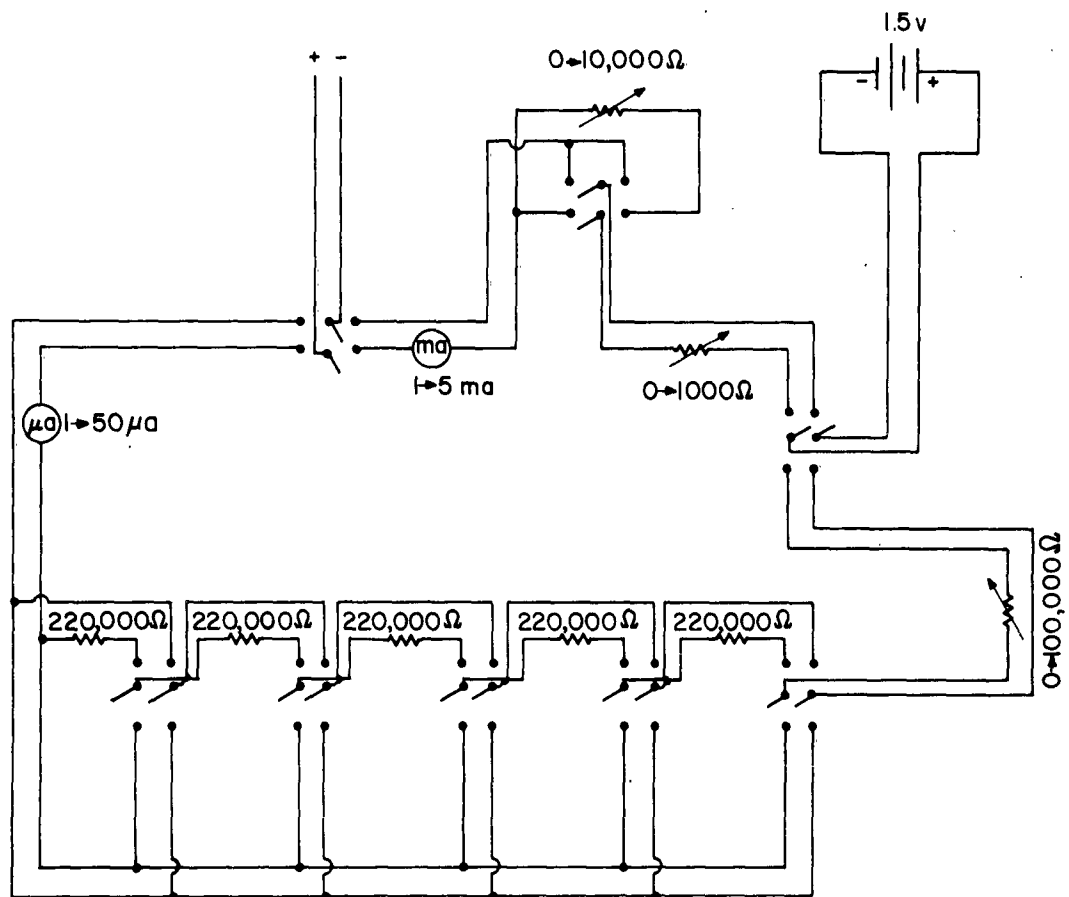


Figure 8: The schematic circuit diagram for the apparatus used to electrolytically etch iron whiskers.

The whisker was etched in a 0.5% aqueous solution of copper-ammoniacal-chloride and examined after periods of 20, 30, and 60 minutes. The current was maintained at  $\sim 50\mu\text{a}$ , giving a current density of about  $\sim 0.3 \text{ amp/cm}^2$ . The etching was carried out in a 100 ml beaker and the cadmium cathode was placed about one inch from the whisker. Metallic copper was observed to come out of solution immediately upon application of the current. Some copper did plate out, but gentle stirring was sufficient to remove much of this copper. The current was always "on" when the whisker was immersed in the etchant. After each period the whisker was rinsed in 1-1 HCl to minimize staining by the copper and finally rinsed in distilled water.

After 20 minutes, examination disclosed some copper deposit and some overgrowth striations. There were some very large pits but no apparent dislocation etch pits. After 30 minutes, very small pits were observed in addition to the very large pits. Also, a channel was observed at the apex of a former tilt boundary. After 60 minutes, the whisker was heavily etched and heavily plated with copper. However, many small and many large pits were seen. The small pits were probably dislocation etch-pits.

#### Whisker Number 2

This was a hexagonal whisker of approximately  $120\mu$  in diameter and about 0.2 cm in length and, hence, had a surface area of  $\sim 8.4 \times 10^{-3} \text{ cm}^2$ . The whisker was somewhat rough and irregular, with one side showing prominent tilt boundaries. A voltage of 1.49 volts was used giving a current of  $30\mu\text{a}$  and a current density of  $\sim 0.3 \text{ amp/cm}^2$ ; a procedure identical to that used for Whisker No. 1 was again used. However, the immersion times in the 0.5% copper-ammoniacal-chloride were changed, periods of  $\frac{1}{2}$ , 1, 1- $\frac{1}{2}$ , and 3 hours being used.

After one-half hour, some large pits were observed but on the whole, corrosion seemed very light. Some small, indistinct pits were observed in isolated areas. After one hour, attack remained light and no distinct etch-pits were observed. After 1- $\frac{1}{2}$  hours, the etching solution became very dark; the attack was somewhat greater and very large, poorly defined pits were noticeable. A fresh solution was made up for the final period. At the end of the final period, the solution was again very dark and "old-looking." After a total of three hours etching time, the whisker shape had not changed much; however, extreme attack was observed in isolated areas. The whisker possessed the general characteristic shape of a  $\langle 111 \rangle$  oriented whisker. There were some very large pits of irregular shape and yet many more very small pits of seemingly rectangular shape. The over-all density of these small pits was very large and their shape was not consistently good. Both the very large and the very small pits are shown in Figs. 9, 10, and 11. One of the more regular large pits was observed more closely. By microscopic examination of the bottom of the pit it was observed that the pit shape was, in fact, a truncated pyramid (Fig. 12).

The results of Whisker No. 2 showed that a lower current density is better; however, the hindrance of the copper plate and the questionable pit shape limit the applicability of this technique. It must be noted that very large specimens were used in this case.

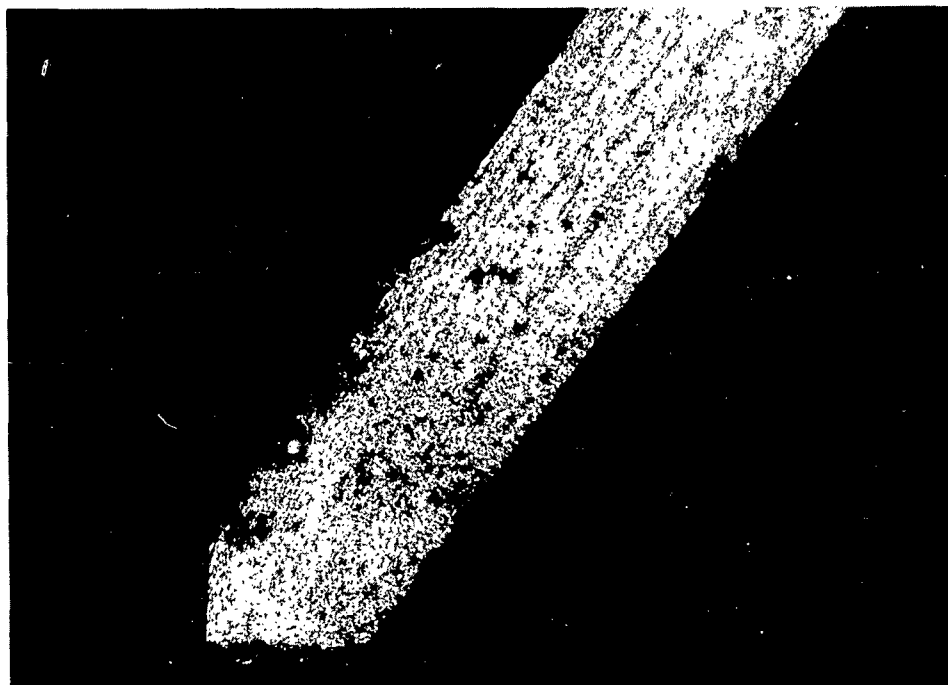


Figure 9. A {110} whisker face after electrolytically etching for 3 hours in 0.5% copper-ammoniacal-chloride at a current density of  $\sim 0.3$  amps/cm<sup>2</sup>; a very large rectangular pit can be seen together with many very small pits. This whisker had  $\langle 111 \rangle$  orientation, was 120 $\mu$  in size, and came from boat No. H-92.

X500

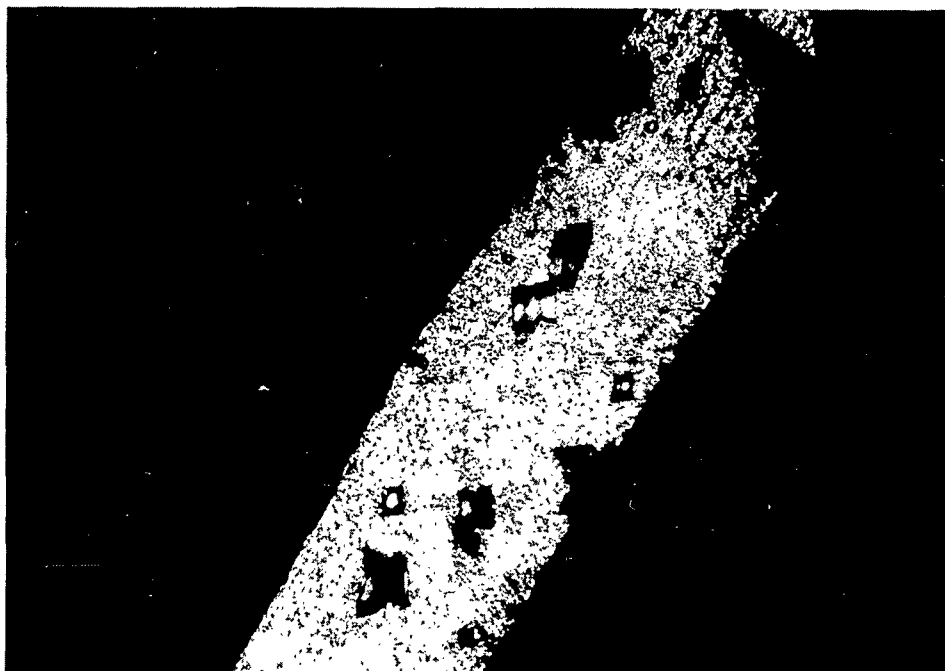


Figure 10. A hexagonal whisker,  $120\mu$  in size, etched for 3 hours electrolytically in 0.5% aqueous copper-ammoniacal-chloride at  $\sim 0.3 \text{ amp/cm}^2$ . This specimen was from boat H-92. Many very large, irregular pits can be observed.

X500



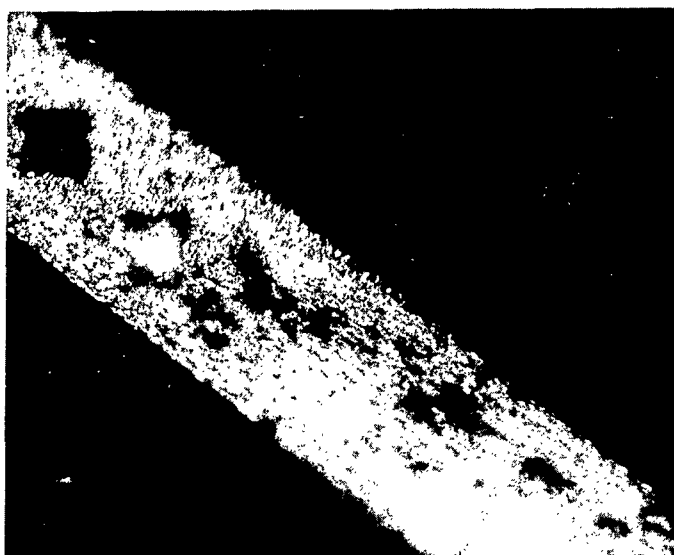


Figure 11. This hexagonal whisker was etched for 3 hours electrolytically in 0.5% copper-ammoniacal-chloride at a current density of  $\sim 0.3$  amps/cm<sup>2</sup>. Whisker size was 120 $\mu$  and the specimen was extracted from boat No. H-92. Very irregular pits were formed at especially active sites.

X500



(a) 500X



(b) 500X

Figure 12. Very large rectangular pits formed by electrolytically etching in 0.5% aqueous copper-ammoniacal-chloride solution for 3 hours at  $\sim 0.3$  amps/cm<sup>2</sup>; (a) focusing at the bottom of the pit shows the truncated-pyramidal shape of the pit; (b) focusing on the {110} face of the whisker. Whisker size was 120 $\mu$  and the orientation was  $\langle 111 \rangle$ . This whisker came from boat No. H-92.

#### D. ETCHING BY HYDROCHLORIC ACID SOLUTIONS

The technique of "dissolution-ledge poisoning" is a powerful tool in the preferential development of relatively contained etch-pits.<sup>11,18,34</sup> A "poison" found satisfactory in many cases is the halide ion and, specifically, chloride ion has proved successful. Gorsuch and Alden<sup>6</sup> reported that some modifications of Fry's<sup>7</sup> reagent were successful in developing etch-pits in iron whiskers. Based upon this suggestion, solutions of concentrated HCl in ethanol containing varying amounts of  $\text{CuCl}_2$  and  $\text{FeCl}_2$  were examined.

The first etchant tested was made up as follows:

100 ml	ethyl alcohol
8 ml	conc. HCl
0.5 gm	$\text{CuCl}_2$
0.2 gm	$\text{FeCl}_2$

(saturate with picric acid).

Whiskers were etched by immersion in a solution that was constantly stirred by means of a magnetic stirrer. After etching, the whiskers were rinsed quickly in 50% hydrochloric acid in ethanol to eliminate any staining due to copper, finally rinsed in distilled water and dried in a blast of hot air. This procedure was followed after every test using HCl. Initially, the {100} faces were attacked very quickly in this etchant and then the rate of corrosion appeared to decrease. These {100} faces were heavily faceted, but the edges remained relatively unattacked. The {110} faces were only slowly attacked, whereas these edges were preferentially removed. Pit density on the {110} faces was much smaller than that on the {100} faces and pit shapes were nearly obliterated as a result of the high rate of attack.

The major portion of the total attack usually occurred within the first 30 seconds of immersion and additional periods of immersion up to five minutes had little effect. However, the severe initial attack made this etchant unsatisfactory for {100} faces. Also, this etchant did not seem to develop pits on {110} faces, especially when both {100} and {110} faces were present as on <110> oriented whiskers.

The second modification of Fry's etchant tested consisted of:

100 ml	ethyl alcohol
8 ml	conc. HCl
0.03 gm	$\text{CuCl}_2$

(saturate with picric acid).

Using the same procedures of immersion, rinsing and drying as in the first case, good etch-pits of reasonably distinct shape were developed on {110} faces of hexagonal, <111>, whiskers. For immersion times greater than about 20 seconds, the etch-pits were no longer contained by the adsorbed poison and lateral dissolution became important. Figure 13 shows a 15 $\mu$



Figure 13. A hexagonal whisker etched for 20 seconds in a modified Fry's reagent containing 0.03 gm  $\text{CuCl}_2$ . Some rectangular pits can be observed, but on the whole, the etch-pits were not well-contained. This whisker was from boat No. 504 and was  $15\mu$  in size.

X500

hexagonal whisker etched in this environment for 20 seconds. The lateral propagation of dissolution-ledges can be observed around many of the etch-pits. This etchant was satisfactory, however, in most experiments.

The third variation of the HCl-based environment consisted of:

100 ml	ethyl alcohol
8 ml	conc. HCl
0.01 gm	CuCl <sub>2</sub>

(saturate with picric acid).

Distinct etch-pits were developed upon immersion times ranging from 5 to 15 seconds on the {110} faces of hexagonal whiskers. With increased etching time, ledges became visible indicating that lateral dissolution of monatomic steps was beginning to occur. Also, the pit shapes became irregular. The optimum etching time was, on the average, approximately 15 seconds in this etchant. For long periods of etching, general corrosion was appreciable but the whisker faces were not heavily attacked, as had occurred in the first case. The pits, however, were not geometrically regular after long periods, except for those pits formed along tilt boundaries. The geometrical shape of these pits persisted after extended periods of etching.

Figure 14 shows a {110} face of a hexagonal whisker etched for five seconds in this etchant. The whisker size was 35 $\mu$  in diameter. Some of the etch-pits formed on this whisker face showed excellent rectangular shapes; however, many more pits had irregular shapes. Figure 15 shows a hexagonal whisker, 30 $\mu$  in diameter, etched for 10 seconds. It can be seen that the over-all attack has increased somewhat, but distinct rectangular etch-pits are still observed on this {110} face. Distinct etch-pits were observed aligned along a tilt boundary and, from the spacing of these pits, the angle of tilt was calculated to be approximately  $1.4 \times 10^{-3}$  degrees (see Appendix I). These etch-pits did, in fact, keep their geometrical shape after continued etching. From these results and other similar tests, it was observed that this modification of Fry's etchant, containing 0.01 gm of CuCl<sub>2</sub>, did develop very satisfactory etch-pits in most cases.

The fourth modification tested contained the following:

100 ml	ethyl alcohol
8 ml	conc. HCl
0.001 gm	CuCl <sub>2</sub>

(saturate with picric acid).

Methods of immersion, rinsing, and drying were again the same as used previously. Experiments showed that good etch-pits were formed at five seconds and remained seemingly unchanged throughout continued etching. Pit density appeared unchanged and the optimum time for best results was again about 15 seconds. General attack was observed after 20 seconds, but for times up to 60 seconds this attack was light. The number of really good, distinct pits was fewer than in the previous case and many large, nondistinct and very small pits were often observed. Figure 16 shows a {110} face of a hexagonal



Figure 14. This whisker, from boat No. R-1, was etched for 5 seconds in Fry's reagent containing 0.01 gm  $\text{CuCl}_2$ . The whisker shape was hexagonal and many distinct, rectangular etch-pits can be observed on the  $\{110\}$  face shown. The size of this whisker was  $35\mu$ .

X500

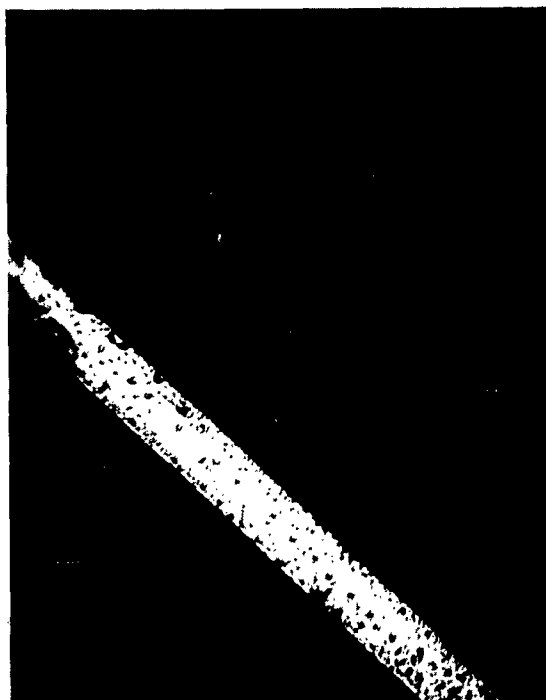


Figure 15. Rectangular etch-pits, aligned along a tilt boundary, were developed on this  $\{110\}$  face of a  $\langle 111 \rangle$  whisker by immersion in a Fry's reagent containing 0.01 gm  $\text{CuCl}_2$  for 10 seconds. This whisker was  $30\mu$  in size and came from boat R-1.

X500



Figure 16. This  $\{110\}$  face of a  $\langle 111 \rangle$  whisker,  $30\mu$  in size, shows distinct rectangular etch-pits. These pits were formed by immersion for 10 seconds in a Fry's reagent containing 0.001 gm of  $\text{CuCl}_2$ . This whisker was extracted from boat No. 504.

X500



whisker. This whisker was 30 $\mu$  in diameter and was etched for 10 seconds. The pit density was very light in some areas and distinct etch-pits were observed as shown in the figure.

Results of the tests using the modified Fry's reagents are summarized in the following table.

Table 1. Compositions of Modified Fry's Reagents

All etchants are based on 8 ml conc. HCl dissolved in 100 ml ethyl alcohol

Weight Added (gm)		Mole-fraction		Optimum Time (sec)	Rating	Remarks
CuCl <sub>2</sub>	FeCl <sub>2</sub>	CuCl <sub>2</sub>	FeCl <sub>2</sub>			
0.05	0.2	2 x 10 <sup>-3</sup>	8 x 10 <sup>-4</sup>	-	Poor	Too severe
0.03	-	1 x 10 <sup>-4</sup>	-	~ 20	Fair-Good	Few good pits
0.01	-	4 x 10 <sup>-5</sup>	-	~ 15	Very Good	Good pits at tilt boundaries
0.001	-	4 x 10 <sup>-6</sup>	-	~ 15	Good	Few good pits

The most serious criticism of these etchants is that the pits formed are usually small and that these pits lose their geometric shape before increasing to a desirable size. However, reasonable confidence can be afforded to these etchants.

#### E. ETCHING BY HYDROFLUORIC ACID SOLUTIONS

In order to study the effectiveness of "poisons" for the development of etch-pits at dislocation sites, the HF-H<sub>2</sub>O-FeF<sub>3</sub> system was chosen as a suitable environment. This system met the requirements for a poison in that a halogen ion of size comparable to the iron lattice was present and that iron and fluorine formed a series of stable complexes. As suggested by Young<sup>11</sup> and Gilman, Johnston, and Sears,<sup>18</sup> the first step was to choose an aqueous HF solution to be used as a base for these etchants. This basic solution should have a dissolution rate of a magnitude which can be appreciably inhibited, by means of poison additions, to a lower optimum dissolution rate at which distinct etch-pits form. Thus, a series of aqueous solutions ranging from 0 to 25 mole-percent HF was investigated.

The procedure used in these tests was to immerse the whiskers in the HF solutions for 60 seconds, during which time the solution was continually stirred. The specimen was then rinsed in distilled water, dried by means of a hot air blast, visually examined and the pitting characteristics carefully noted. Dissolution rates were determined by chemically analyzing for the iron pick-up in the etching environments and relating this to the thickness of iron removed. A colorimetric technique was used to quantitatively measure the iron pick-up. The Fe<sup>+++</sup> color was developed using 1,10-phenanthroline and the transmittancy read using a Coleman spectrophotometer. With careful

preparation of blanks and accurate calibration of the instrument, the maximum error in the chemical analysis would be about 1%. However, the determination of the surface area of the whiskers, which was measured with an optical microscope, was much less accurate, with a maximum probable error of about 10%. A sample calculation of the dissolution rate as determined in these studies is presented in Appendix II.

The results of these studies are summarized in Fig. 17. It was found that the dissolution rates were low, probably due to the weakly acidic nature of the HF acid. For concentrations above 10 mole-percent the whiskers were unattacked. The accuracy of the measurements was verified by means of independent determinations on various whiskers at representative concentrations of 3.0 and 7.0 mole-percents; these results were in close agreement. Pitting attack was generally nondescript in these etchants. It must be noted, however, that large whiskers,  $\sim 100\mu$ , were used in order to more accurately measure the surface areas. The 0.5 mole-percent aqueous HF solutions showed a tendency toward distinct pit formation but had very low dissolution rates. Thus, these solutions did not lend themselves to the scheme of dissolution control by means of poison additions. Figure 18 shows a square whisker,  $\sim 80\mu$  in size, etched in 9.0 mole-percent HF solution for 15 seconds. Pits can be seen along a tilt-boundary, but these pits are mostly nongeometric due to excessive lateral dissolution.

The base concentration for the "FeF<sub>3</sub>-poisoned" etchants was chosen to be 3.0 mole-percent because this resulted in the maximum dissolution rate, viz.,  $\sim 4\mu/\text{min}$ , and would be expected to show the effects of poison inhibition. The 3.0 mole-percent aqueous solutions of HF contained 0 to  $10^{-5}$  mole-fraction of FeF<sub>3</sub>. These environments were studied in a manner identical to the HF-H<sub>2</sub>O environments used above and again the dissolution rates were determined by means of chemical analyses. Results of these tests, together with representative etch-pit figures, are shown in Fig. 19. These results show a linear decrease of dissolution rate with increasing concentration of FeF<sub>3</sub> in solution, at least over the range examined. All these etchants poisoned with FeF<sub>3</sub> produced discernable pits, as observed in Fig. 19. Particularly good pits were developed using etchants containing  $6.5 \times 10^{-8}$  mole-fraction of FeF<sub>3</sub>. Descriptions of the whiskers used in Fig. 19 are given in Table 2. Note that these whiskers were all etched in 3.0 mole-percent aqueous HF containing the indicated amounts of FeF<sub>3</sub>.

Table 2. Description of whiskers shown in Fig. 19 used to study the dissolution rates of aqueous HF solutions poisoned with FeF<sub>3</sub>

Mole-fraction FeF <sub>3</sub>	Mole-fraction FeF <sub>3</sub> Hydrate	Orientation	Boat No.	Whisker Size	Etching Time
$6.5 \times 10^{-8}$	$10^{-7}$	< 111 >	504	30 $\mu$	60 sec.
$6.5 \times 10^{-7}$	$10^{-6}$	< 111 >	504	25 $\mu$	60 sec.
$6.5 \times 10^{-6}$	$10^{-5}$	irregular	539	20 $\mu$	60 sec.
$6.5 \times 10^{-5}$	$10^{-4}$	< 111 >	504	26 $\mu$	60 sec.

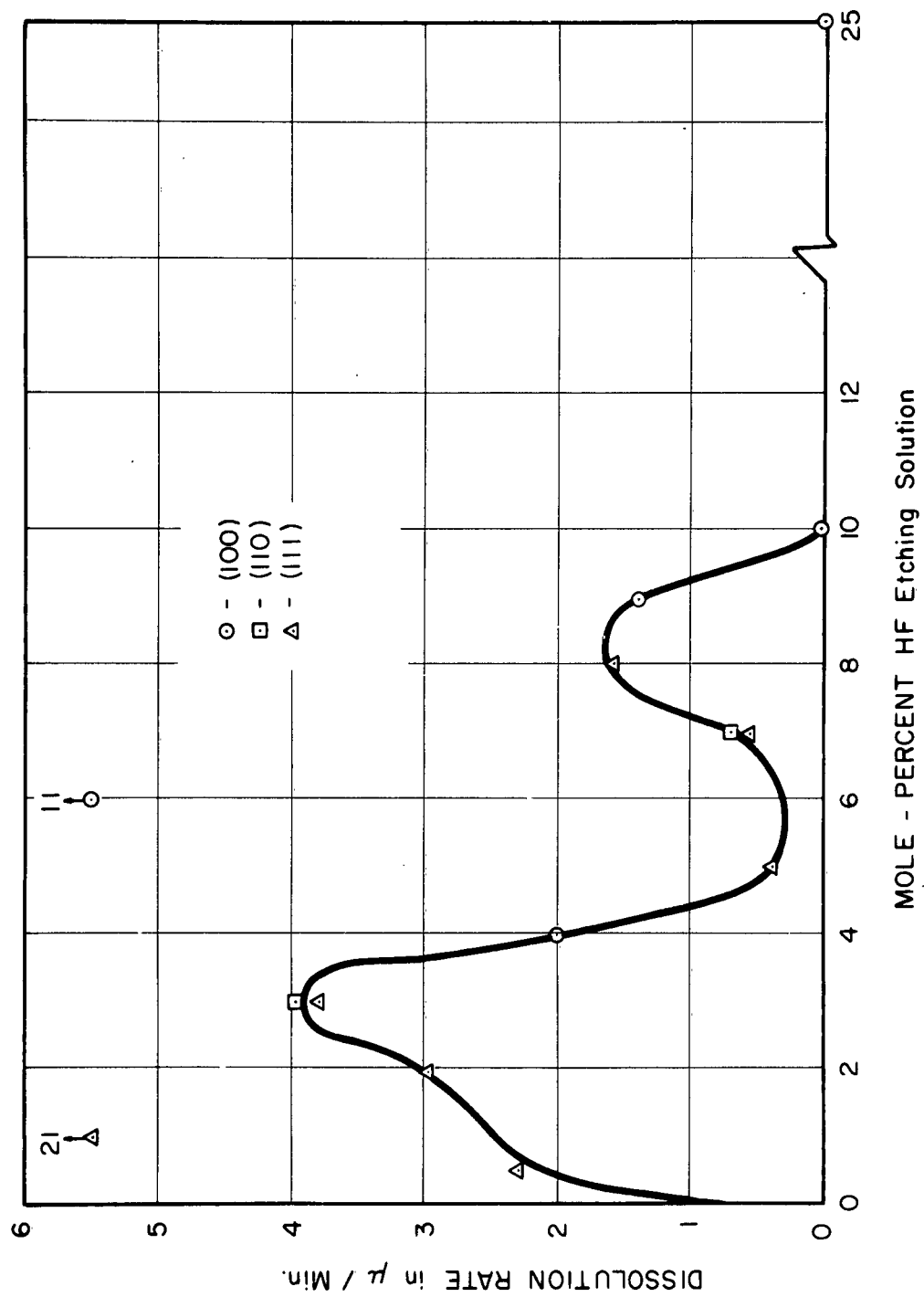


Figure 17: Dissolution rate of iron whiskers of various growth orientations as a function of HF conc. in water.

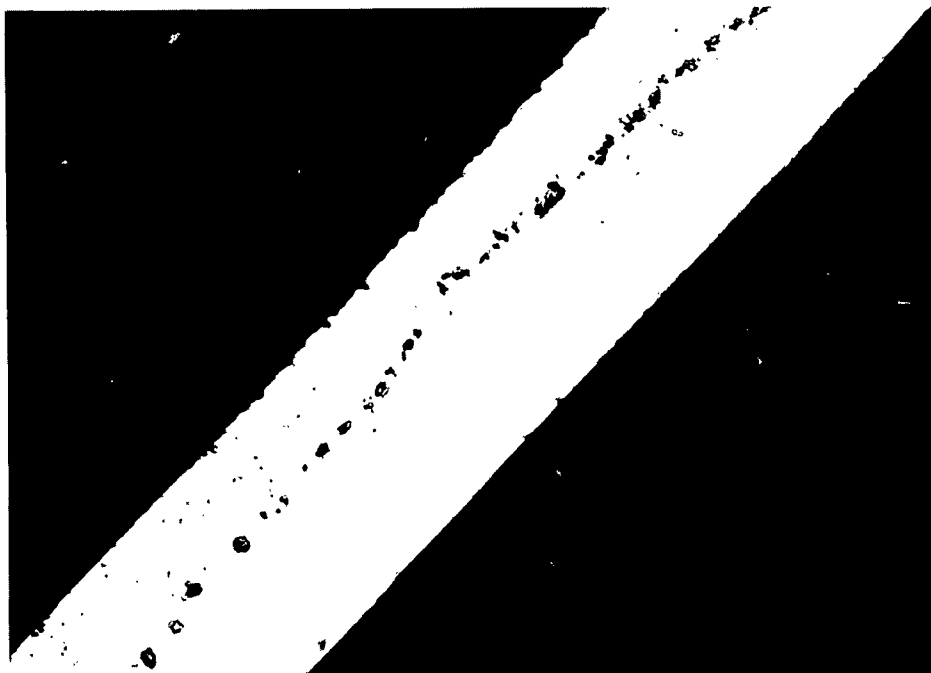


Figure 18. Dissolution at dislocation sites along a tilt-boundary produced by etching in 9.0 mole-percent HF acid solution in water for 15 seconds; the dissolution rate was  $1.6 \mu/\text{minute}$ . This whisker was  $80\mu$  in size, square, and extracted from boat No. H-93. Some very small, square etch-pits are still visible.

X500

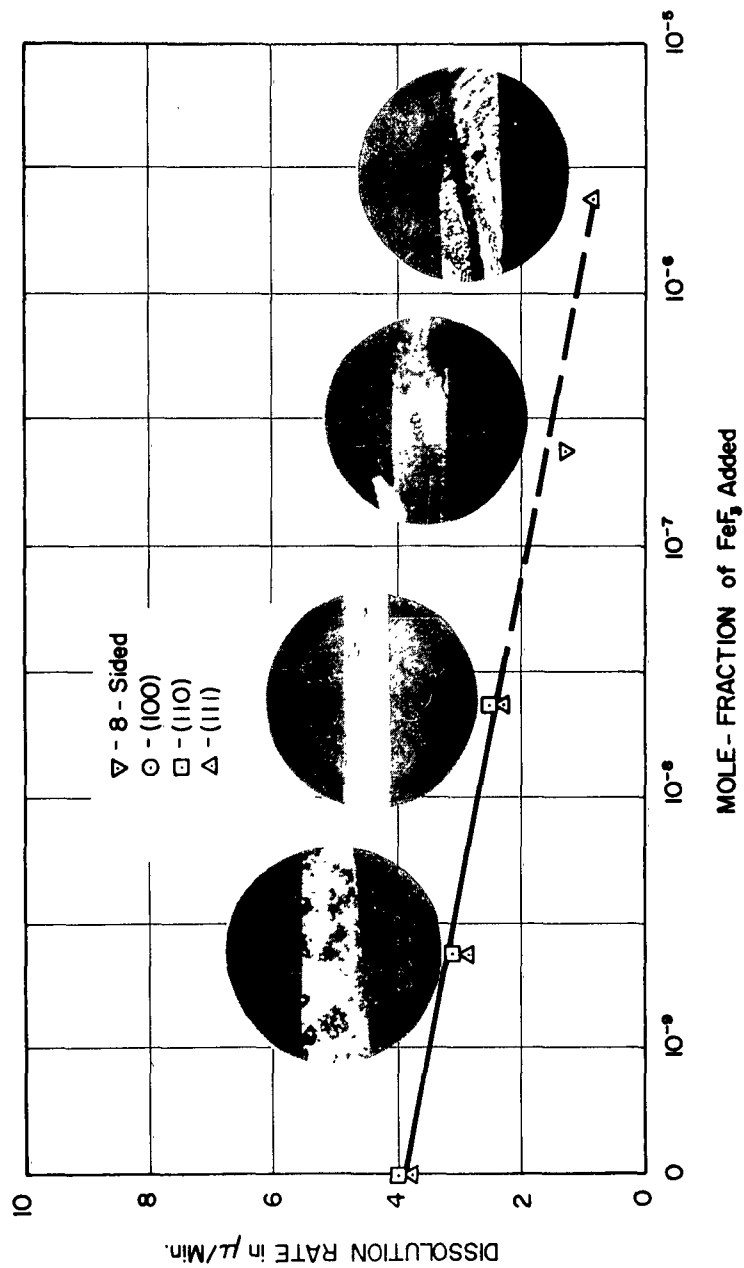


Figure 19. Dissolution rate of iron whiskers of various growth orientations etched in 3.0 mole-percent HF solution in water as a function of the conc. of  $\text{FeF}_3$  hydrate ( $\text{Fe} = 31.21\%$ ) poison used.

The whisker shown in Fig. 20 was etched for 60 seconds in 3.0 mole-percent HF containing  $6.5 \times 10^{-7}$  mole-fraction of  $\text{FeF}_3$ . This was a rectangular whisker of  $40\mu$  size showing the {100} face. Dissolution pits can be noted on this whisker face; however, in this case, the dissolution ledges were not well contained.

The  $\text{FeF}_3$  used in these tests was purchased from the K and K Laboratories, Inc., Jamaica, New York. Analyses of this ferric-fluoride hydrate are given in Table 3.

Table 3. Ferric Fluoride Analyses

Constituent	Manufacturer's ( $\text{FeF}_3 \cdot 4.5 \text{ H}_2\text{O}$ )	In this Laboratory ( $\text{FeF}_3 \cdot 3.7 \text{ H}_2\text{O}$ )
Fe	28.8%	31.2%
F <sub>2</sub>	29.4%	32.0%
H <sub>2</sub> O	41.8%	36.8%

The analyses performed at this laboratory were done by means of titration with  $\text{TiCl}_3$  using  $\text{NH}_4\text{SCN}$  indicator which turns red in the presence of  $\text{Fe}^{+++}$ , according to the reaction,



Upon reduction of the  $\text{Fe}^{+++}$  ion, the indicator turned from red to clear. These analyses showed that the  $\text{FeF}_3$ -hydrate had, in fact, lost some water content from the time of manufacture. Therefore, all calculations of the mole-fraction of hydrate and of  $\text{FeF}_3$  (anhydrous) were based upon the hydrate form of  $\text{FeF}_3 \cdot 3.7 \text{ H}_2\text{O}$ . This analysis was also checked colorimetrically using the previously described procedure.

The results of the determinations of the dissolution rates are given in Table 4.

#### F. ETCHING BY SULFURIC ACID SOLUTIONS

An etch designed to study the dislocation structure of iron whiskers should form etch pits only at dislocation sites, produce minimum background attack, and cause the whisker to be reduced uniformly in cross section but not so rapidly that observations cannot be made. These conditions have been satisfactorily met by using the etch  $1\text{N H}_2\text{SO}_4 + 0.2\text{N K}_2\text{S}_2\text{O}_8$ . A rate of penetration of about  $0.33 \mu/\text{min}$  ( $15 \text{ ma}/\text{cm}^2$ ) was measured perpendicular to the {100} face of one large square and one large rectangular whisker. This rate was calculated from the reduction in thickness of the whiskers during etching. This  $1\text{N H}_2\text{SO}_4 + 0.2\text{N K}_2\text{S}_2\text{O}_8$  solution creates a dissolution rate intermediate



Figure 20. A rectangular whisker etched in 3.0 mole-percent HF in water and containing  $6.5 \times 10^{-7}$  mole-fraction of  $\text{FeF}_3$ . The immersion time was 60 seconds and the whisker was taken from boat No. 539; the size was  $40\mu$ . Dissolution ledges are quite distinct on {100} face shown here. The dissolution rate was  $2.5\mu/\text{minute}$ .

X500

Table 4. Summary of Dissolution Rates

Whisker Used			Etchant		Dissolution Rates	
Shape	Size	Boat No.	HF	FeF <sub>3</sub>	$\mu/\text{min}$	$\text{Mg}/\text{min.cm}^2$
	( $\mu$ )		(mole-%)	(mole-fract)		
< 111 >	115	H-93	0.5		2.3	1.8
< 111 >	200	H-93	2.0		3.0	2.5
< 111 >	30	504	3.0		3.8	3.0
< 110 >	85	H-93	3.0		4.0	2.9
< 100 >	60	H-93	4.0		2.0	1.6
< 111 >	120	H-93	5.0		0.4	0.3
< 100 >	100	H-93	6.0		11.2***	8.8
< 110 >	45	H-93	7.0		0.7	0.6
< 111 >	115	H-93	7.0		0.6	0.5
< 111 >	115	H-93	8.0		1.6	1.3
< 100 >	80	H-93	9.0		1.4	1.1
< 100 >	130	H-93	10.0		Nil	Nil
< 100 >	170	H-93	25.0		Nil	Nil
< 111 >	17	504	3.0	$6.5 \times 10^{-8}$	2.9	2.3
< 110 >	25	539	3.0	$6.5 \times 10^{-8}$	3.1	2.4
< 111 >	25	504	3.0	$6.5 \times 10^{-7}$	2.4	1.9
< 110 >	40	539	3.0	$6.5 \times 10^{-7}$	2.5	2.0
< 111 >	30	504	3.0	$6.5 \times 10^{-8}$	2.7*	2.1
~< 110 >	20	539	3.0	$6.5 \times 10^{-8}$	1.3**	
< 111 >	9	539	3.0	$6.5 \times 10^{-5}$	0.9**	

\*Due to high FeF<sub>3</sub> content, a dilution of 25:1 was required in order to bring the Fe<sup>+++</sup> in the range of the spectrophotometer and hence the error involved is greatly increased.

\*\*Dissolution rates measured optically.

\*\*\*Contamination led to high results.



between that found for the solution  $1N H_2SO_4 + 0.02N K_2S_2O_8$  and the solution  $1N H_2SO_4 + 0.5N (NH_4)_2S_2O_8$ . The rate of penetration was measured on whiskers which developed relatively shallow etch pits. The calculation of corrosion rate in this manner cannot be applied directly to a surface containing large, well defined pits, such as illustrated in Fig. 21.

Figure 21 shows pits formed on the  $\{100\}$  face of a rectangular iron whisker using the  $1N H_2SO_4 + 0.2N K_2S_2O_8$  etchant. The pits were bounded by approximately  $\{110\}$  side-faces and had a  $\{100\}$  bottom. This was verified by measuring the width and depth of the pits and calculating the angle of intersection between the pit faces and the  $\{100\}$  surface.

The pits shown in Fig. 21 were correctly oriented for a growth axis of  $<110>$  which is expected for rectangular whiskers. Once it has been established that the  $1N H_2SO_4 + 0.2N K_2S_2O_8$  etchant does in fact preferentially create pits delineated by  $\{110\}$  planes, then whisker faces containing fairly small but well defined pits can be oriented by a visual examination of the pitted surface.

Figure 22a shows another example of large well-developed etch pits present on a  $\{100\}$  surface of a rectangular whisker after etching for  $1\frac{1}{2}$  minutes. Most of the surface was composed of interlocking pits. Some of the pit bottoms have united to form larger, flat-bottom areas. After etching for  $2\frac{1}{2}$  minutes, Fig. 22b, no individual pits were present. It is assumed that the pit-sides continued to expand rapidly, until the original surface was completely removed. A few remaining portions of the original surface can still be seen in Fig. 22b. This type of etching can occur only if the outside layer is of uniform thickness and in some manner dissimilar to the inside core of the whisker. It was concluded that whiskers can be composed of an outside shell and an inside core region. Weik<sup>35</sup> has also reported the existence of a shell and a core based on tensile tests. The shell often ruptured before the core.

Etch-pits in the shell of most rectangular whiskers were smaller than those shown in Figs. 21a and 22b. This was because the shell on these whiskers was thinner. Not every whisker had a shell and core. Two plate-like whiskers, several microns thick, appeared to have as-grown dislocations extending through the whisker perpendicular to the broad face. Adjacent to those pits which etched through the whisker were many pits with flat-bottoms, suggesting a shell and core in this portion.

Square and hexagonal whiskers also have a shell and core although the shell was never as thick as that found in Figs. 21a and 22a. Figure 23 shows pits in the shell of a square whisker. A  $5\mu$  square whisker was the smallest whisker in which a shell and a core were definitely observed. Etch-pits were observed on whiskers as small as  $1\mu$ , Fig. 24. Not every whisker had as-grown dislocations intersecting the surface. One  $2.5\mu$  square whisker was etched for 10 minutes in  $1N H_2SO_4 + 0.2N K_2S_2O_8$  and showed no etch-pits and very little attack of any kind. Probably no dislocations intersected this surface. Etch-pits formed on the  $\{110\}$  face of hexagonal whiskers were usually less clearly defined, Fig. 25. When this shell was removed, the etch-pits that formed in the core were very shallow.

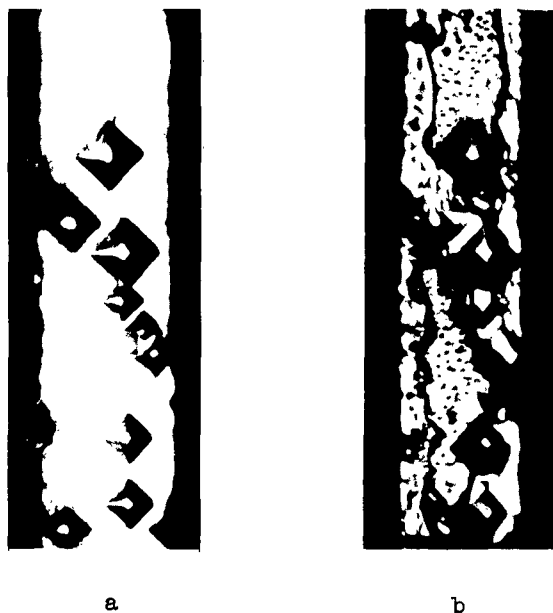


Figure 21. Etch pits at as-grown and deformation dislocations.

Rectangular whisker, (100) face, from boat H-121.

- a) Etched for 1-1/2 min in 1N  $\text{H}_2\text{SO}_4$  + 0.2N  $\text{K}_2\text{S}_2\text{O}_8$ . 1000X
- b) Deformed after the 1-1/2 min etch, then etched for 1 additional minute. 1000X



Figure 22. Removal of whisker shell.

Rectangular whisker, (100) face, from boat H-121.

- a) Etched for 1-1/2 min in 1N  $\text{H}_2\text{SO}_4$  + 0.2N  $\text{K}_2\text{S}_2\text{O}_8$ . 1000X
- b) Same area as in (a) except etched for an additional minute 1000X

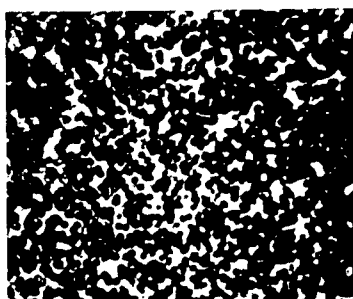


Figure 23. Etching of whisker shell.

Square whisker, from boat 529.

Etched for 2 min in 1N  $\text{H}_2\text{SO}_4$  + 0.2N  $\text{K}_2\text{S}_2\text{O}_8$ . 1000X

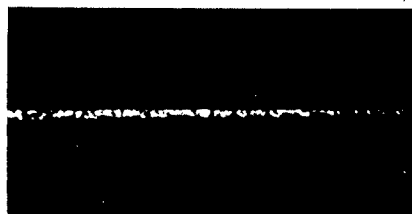


Figure 24. Etch pits at as-grown dislocations.

Square whisker, from boat 538.

Etched 1-1/2 min in 1N  $\text{H}_2\text{SO}_4$  + 0.2N  $\text{K}_2\text{S}_2\text{O}_8$ . 1000X

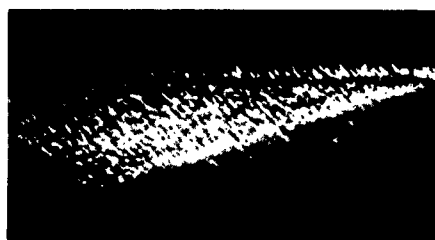


Figure 25. Etching of whisker shell.

Hexagonal whisker, from boat H-89.

Etched for 1/2 min in 1N  $\text{H}_2\text{SO}_4$  + 0.2N  $\text{K}_2\text{S}_2\text{O}_8$ . 1000X

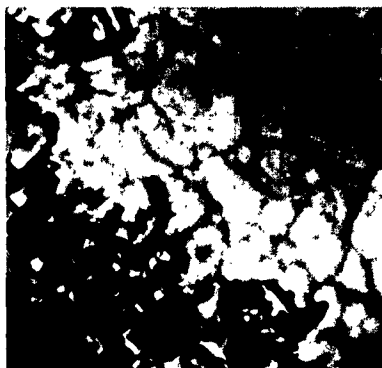
Etch-pits at clean dislocations resulting from deformation had similar appearance to those at as-grown dislocations. The deformed whiskers were bent so that the radius of bending was normal to the growth axis and approximately perpendicular to the face being examined. The small pits in the background of Fig. 21b were formed at deformation dislocation sites. The etch pits at the as-grown dislocations were much larger, but this was probably because of a longer dislocation line and longer etching time. Pits at both types of dislocations were well defined. There is no evidence to suggest that the as-grown dislocations moved during deformation. Impurity atoms segregated along the as-grown dislocations probably pinned these dislocations and prevented them from moving under a stress sufficient to cause the movement of clean dislocations.

Figure 26a shows a plate-like whisker in which the shell and the core were present simultaneously. Etch-pits in the shell were well-defined, having a regular crystallographic shape. Dislocations in the core etched as very wide, shallow pits. After deforming the whisker and re-etching, very small, shallow pits etched at the deformation dislocation sites, Fig. 26b. Another similar example is shown in Fig. 27. The unusual dislocation structure in the shell was removed completely with continued etching, leaving a smooth core. The etch-pits produced at as-grown dislocations in the core were so wide and shallow that they were barely visible. After deforming the whisker and re-etching, the pits were still very shallow although slightly better defined. When the pits at as-grown dislocations were shallow and without crystallographic shape, the pits at deformation dislocations were also shallow and pock-like. Pits at deformation dislocations were well-defined in a layer in which the as-grown dislocations were also well-defined.

Etch-pits at deformation dislocations in the core of a hexagonal whisker are shown in Fig. 28. Prior to deformation the core was smooth with only a slight suggestion of etch-pits. The pit bottoms were asymmetric indicating that the dislocation lines were not perpendicular to the surface in this case. Figure 28a shows large, pock-like pits on the center surface which had a {110} orientation, while the plane at a low angle to the {110} face on the left side contained small well-contained pits. Deeper within the whisker, Fig. 28b, asymmetric pits with crystallographic shape were formed, again on a face at a low angle to the {110}. Etch-pits at deformation dislocations on {110} faces in the core of most hexagonal whiskers were not as clearly defined as these pits.

The 4% picral solution was usually ineffective in forming pits at as-grown dislocations on {100} faces. Some dissolution was probably occurring even when no pits were formed. A short etch in  $1N H_2SO_4 + 0.2N K_2S_2O_8$  formed pits on those whiskers which did not pit in 4% picral. Figures 29a and 30a show two illustrations which suggest that, on hexagonal whiskers, 4% picral and 2% nitral preferentially create rectangular pits bounded by two {100} planes. No pits were found which were deep enough to measure the angle of intersection of the pit faces with the surface. After extended etching, both the picral and nitral caused considerable background etching, Figs. 29b and 30b. A short etch in  $1N H_2SO_4 + 0.2N K_2S_2O_8$  completely removed this shell and left the core smooth with only a slight suggestion of possible pitting, Figs. 29c and 30c. The density of etch-pits shown in Figs. 29a and 30a was

a



b



Figure 26. Etched pits at as-grown and deformation dislocations in whisker core.

Plate-like whisker, (100) face, from boat H-75.

- a) Etched for 9 min in 1N  $\text{H}_2\text{SO}_4$  + 0.2N  $\text{K}_2\text{S}_2\text{O}_8$ . 1000X
- b) Deformed after etching for 9 min, then etched for 8 min following deformation. 1000X

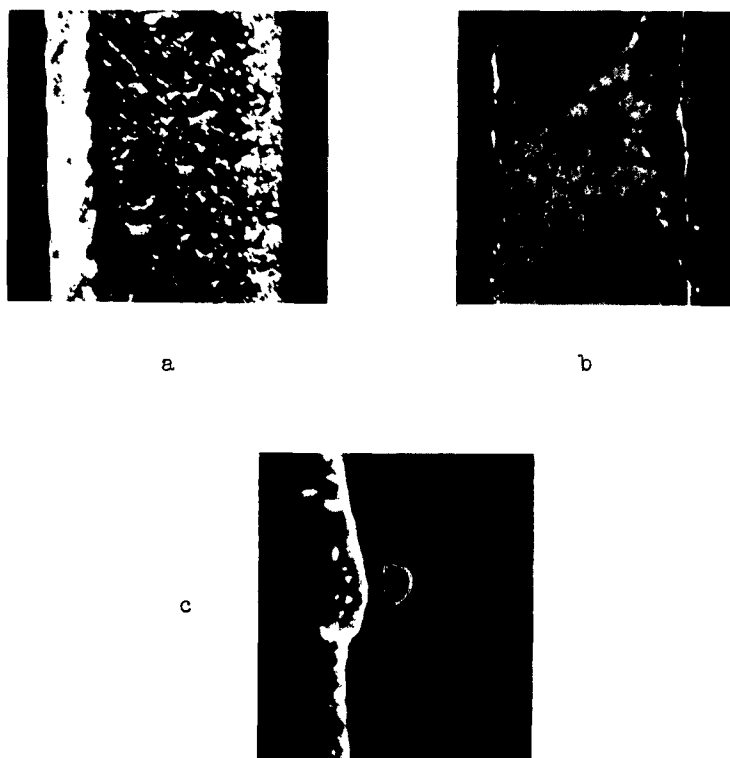


Figure 27. Removal of whisker shell.

Rectangular whisker,  $\{100\}$  face, from boat H-121.

- a) Etched for 1 min in  $1N\ H_2SO_4 + 0.2N\ K_2S_2O_8$ . 1000X
- b) Same as (a) except etched for 6-1/2 min.
- c) Deformed after etching 6-1/2 min and then etched for an additional 5 min. 1000X



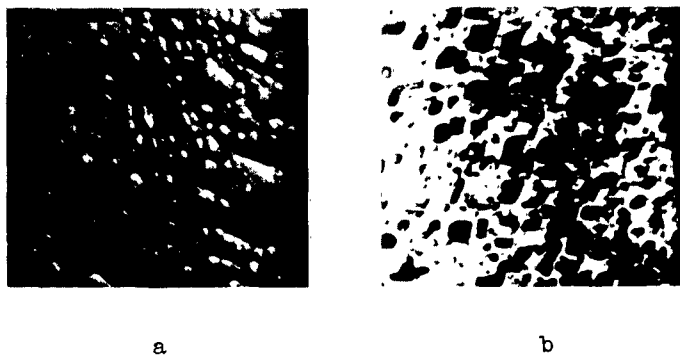


Figure 28. Etching of the core of a deformed whisker.

Hexagonal whisker, from boat H-89.

- a) Deformed after etching 4 min in  $1\text{N H}_2\text{SO}_4 + 0.2\text{N K}_2\text{S}_2\text{O}_8$  and then re-etched for 10 min following deformation. 1000X
- b) Same as (a) except etched for 16 min following deformation.

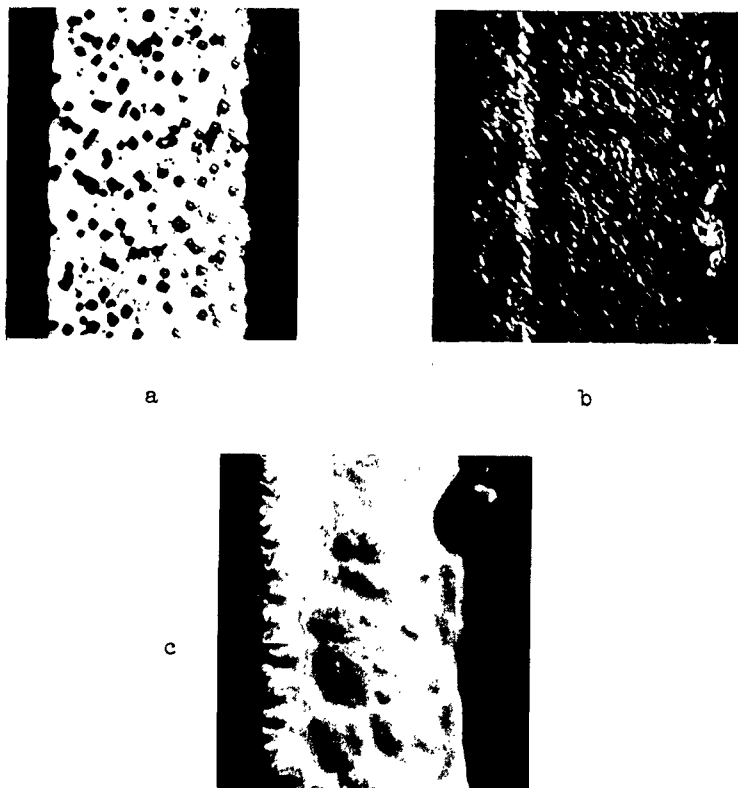


Figure 29. Removal of whisker shell.

Hexagonal whisker, from boat H-91.

- a) Etched for 5 min in 4% picral. 1000X
- b) Etched for 45 min in 4% picral. 1000X
- c) Etched for 45 min in 4% picral followed  
by 1-1/2 min etch in 1N  $\text{H}_2\text{SO}_4$  + 0.2N  $\text{K}_2\text{S}_2\text{O}_8$ . 1000X

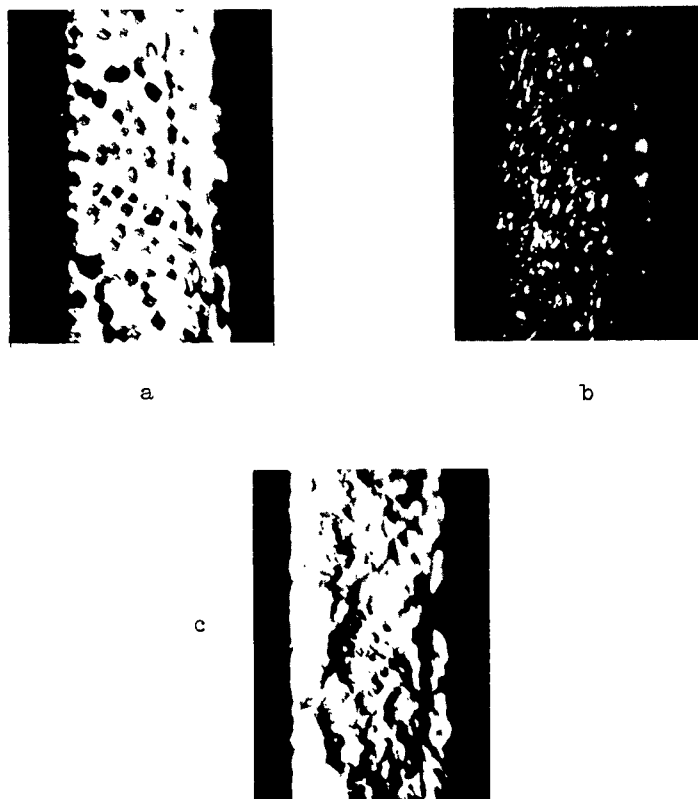


Figure 30. Removal of whisker shell.

Hexagonal whisker, from boat H-91.

- a) Etched for 4 min in 2% nital. 1000X
- b) Same as (a) except etched for 10 min.
- c) Etched as stated in (b) followed by 1/2 min etch in  
 $1N\ H_2SO_4 + 0.2N\ K_2S_2O_8$ . 1000X

normally found. Figure 3la shows a hexagonal whisker with a very high as-grown dislocation density. Regardless of the dislocation density, the picral and nital produced better-defined pits on hexagonal whiskers than did the 1N  $H_2SO_4$  + 0.2N  $K_2S_2O_8$  etchant. Figure 3lb shows the core after removal of the shell shown in Fig. 3la. No etch-pits were present after etching the core in 4% picral. Fig. 3lc. A very high as-grown dislocation density was revealed after a short etch in 2% nital, Fig. 3ld. A subsequent etch in 1N  $H_2SO_4$  + 0.2N  $K_2S_2O_8$  removed these pits.

The shell and the core did not always have the same orientation. Rectangular whiskers normally have a  $\langle 110 \rangle$  growth axis, and yet the shell covering the broad face of three rectangular whiskers was found to be a  $\{100\}$  plane rotated into a  $\langle 100 \rangle$  growth axis. The interface between the shell and the core represented a twist boundary of  $45^\circ$  rotation. The  $\{110\}$  side planes of these whiskers were poorly developed which indicated that the rectangular shape of these whiskers probably resulted from a  $\langle 110 \rangle$  growth axis of the core. This rotation was determined by the orientation of etch-pits on two of these whiskers. Figure 32 shows etch pits in the shell of one of these whiskers. Based on the assumption that these pits were outlined by  $\{110\}$  faces, their orientation corresponded to a  $\langle 100 \rangle$  growth axis. Etch-pits in the core were too small for orientation determination. The second whisker which showed this rotation had small, but well-defined pits in both the shell and the core. A change in orientation of the pits between the shell and core could be observed. On the third whisker the growth axis of the shell was determined from the slip lines present on the shell after deformation. Opinsky and Smoluchowski<sup>38</sup> indicated that, based on the critical, resolved shear stress, the  $(1\bar{1}2)[\bar{1}11]$  and the  $(2\bar{1}3)[\bar{1}11]$  slip system are favored for a square  $\langle 001 \rangle$  whisker and the  $(\bar{3}12)[111]$  and  $(\bar{2}11)[111]$  systems for a rectangular  $\langle 011 \rangle$  whisker. The two sets of slip lines observed on this whisker agreed with the traces of  $(1\bar{1}2)$  and  $(2\bar{1}3)$  planes assuming a  $\langle 001 \rangle$  growth axis. These correlations, together with the above, warrant confidence in these  $H_2SO_4$  -  $K_2S_2O_8$  etchants for the formation of etch-pits at dislocation sites.

#### IV. DISCUSSION

##### A. COPPER-AMMONIACAL-CHLORIDE

It has been demonstrated that good etch pits can be developed by aqueous solutions of copper-ammoniacal-chloride; however, these results are severely limited in most cases by (1) the small size of the pits, and (2) the covering of the whisker surface by a layer of "spongy" copper. It must be noted that this etchant was intended to be a macro-etchant, where the "spongy" layer could be tolerated since it would be no problem to wipe it from the etched surface.

The etch pits observed on whiskers immersed in 2% copper-ammoniacal-chloride were seen to be aligned in approximately the same direction on a given whisker. The pits were observed in many cases to have pyramidal shapes, Fig. 4, very similar to etch pits developed at dislocation sites

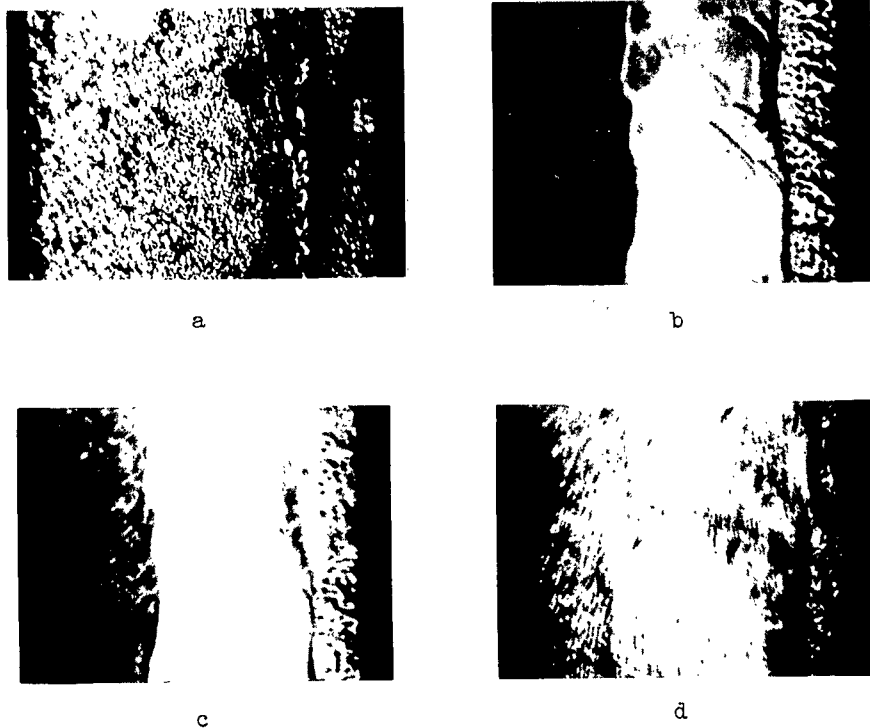


Figure 31. Removal of whisker shell.

Hexagonal whisker, from boat H-91.

- a) Etched for 4 min in 4% picral. 1000X
- b) Etched for 45 min in 4% picral, and then 5 min in 1N  $H_2SO_4$  + 0.2N  $K_2S_2O_8$ . 1000X
- c) Etched as stated in (b) followed by a 4 min etch in 4% picral. 1000X
- d) Etched as stated in (c) followed by a 3 min etch in 2% nital. 1000X

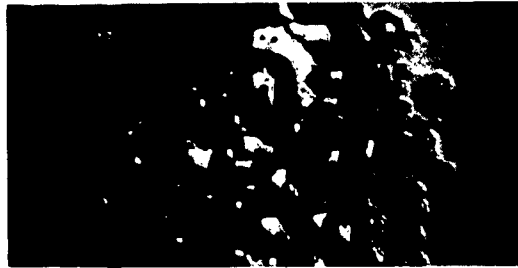


Figure 32. Rotation of shell and core.

Rectangular whisker, (100), face from boat H-121.

Etched for 4-1/2 min in 1N  $\text{H}_2\text{SO}_4$  + 0.2N  $\text{K}_2\text{S}_2\text{O}_8$ . 1000X

in ionic crystals.<sup>34,12</sup> A more convincing proof that these pits formed on the iron whiskers do, in fact, correspond to dislocation sites can be presented by analysis of the pit alignment. Using Fig. 4, the angles of inclination with the edge of the whisker faces, a  $\langle 111 \rangle$  direction since these were hexagonal whiskers, was measured and two prominent angles were obtained,  $\sim 40^\circ$  and  $\sim 55^\circ$ , the  $55^\circ$  being the more prominent. Three possible sites of slip planes are possible in bcc iron,  $\{110\}$ ,  $\{112\}$ , and  $\{123\}$ , and of these three it can be found that  $\{110\}$  and  $\{123\}$  made angles with  $\{111\}$  of  $35.3^\circ$  and  $51.9^\circ$ , respectively.<sup>37</sup> Since a  $\langle 111 \rangle$  direction is perpendicular to a  $\{111\}$  plane, these planes,  $\{110\}$  and  $\{123\}$ , make angles of  $54.7^\circ$  and  $38.1^\circ$ , respectively, with a  $\langle 111 \rangle$  direction. This is in excellent agreement with the angles measured. The slip systems developed in these cases would, therefore, be  $\{110\} \langle 111 \rangle$  and  $\{123\} \langle 111 \rangle$ . Another more qualitative proof of the existence of true dislocation etch pits was the observation that neither the pit size nor the pit density increases with time of immersion. This would be expected for dislocation etch pits. There was no method of determining if all dislocations were developed since much of the whisker faces was covered by means of "plated-out" copper. Again this plating phenomenon turns out to be an important shortcoming.

Additional proof concerning the reliability of the above etch-pitting technique was demonstrated by using a slightly deformed whisker. The whisker, a  $\langle 100 \rangle$  oriented whisker approximately  $14\mu$  in size, was bent slightly before etching. After etching for one hour in 2% copper-ammoniacal-chloride, pits were formed that could be interpreted as dislocation etch-pits (Fig. 6). For an  $\alpha$ -Fe crystal, the possible slip systems are  $\{110\} \langle 111 \rangle$ ,  $\{112\} \langle 111 \rangle$ , and  $\{123\} \langle 111 \rangle$ . Referring to a stereographic projection showing the principal unit triangle and the main slip systems operative,<sup>38</sup> it can be seen that, since this was a  $\langle 100 \rangle$  oriented whisker, one would expect systems of the type  $\{112\} \langle 111 \rangle$  or  $\{123\} \langle 111 \rangle$  to operate because these surround the center pole, a  $\{100\}$  type, Fig. 33. From the photomicrograph, slip lines were found to intersect the  $\{100\}$  face (shown on edge in Fig. 6) at angles from  $15^\circ$ - $25^\circ$ . Possible orientations for this slip system are shown in Fig. 34b. Figure 34a shows the intercepts of  $\{112\}$  and  $\{123\}$  with a  $\{100\}$  face and the angles of intersection were calculated, (see Appendix III). Since the lines shown in the photomicrograph were irregular, this suggests that multiple slip had occurred, and from the unit triangle (Fig. 33), the  $\{112\} \langle 111 \rangle$  and  $\{123\} \langle 111 \rangle$  systems should have been approximately equally favored. The intercepts of the  $\{112\}$  and  $\{123\}$  were shown to make angles of the same magnitude as actually measured. It was concluded that slip had occurred on these systems, indicating that the etchant had, in fact, developed etch pits outlining the traces of these slip planes. Note here that etchants involving  $\text{CuCl}_2$  are noted for developing strain lines.

Since slip had occurred, the absence of distinct, single etch pits can be explained. The consequence of the dislocations formed upon deformation is shown schematically in Fig 34c assuming the slip system  $(112)[111]$ , it can be seen that the dislocation loops could have slipped out at the edge and formed the slip lines. However, at the corner, dislocations would be present and would etch out in the presence of a satisfactory environment. Examination of Fig. 6 showed, indeed, a channel etched along the edge of an otherwise uniformly pitted whisker face. Therefore, a strong verification does exist for the above discussion.





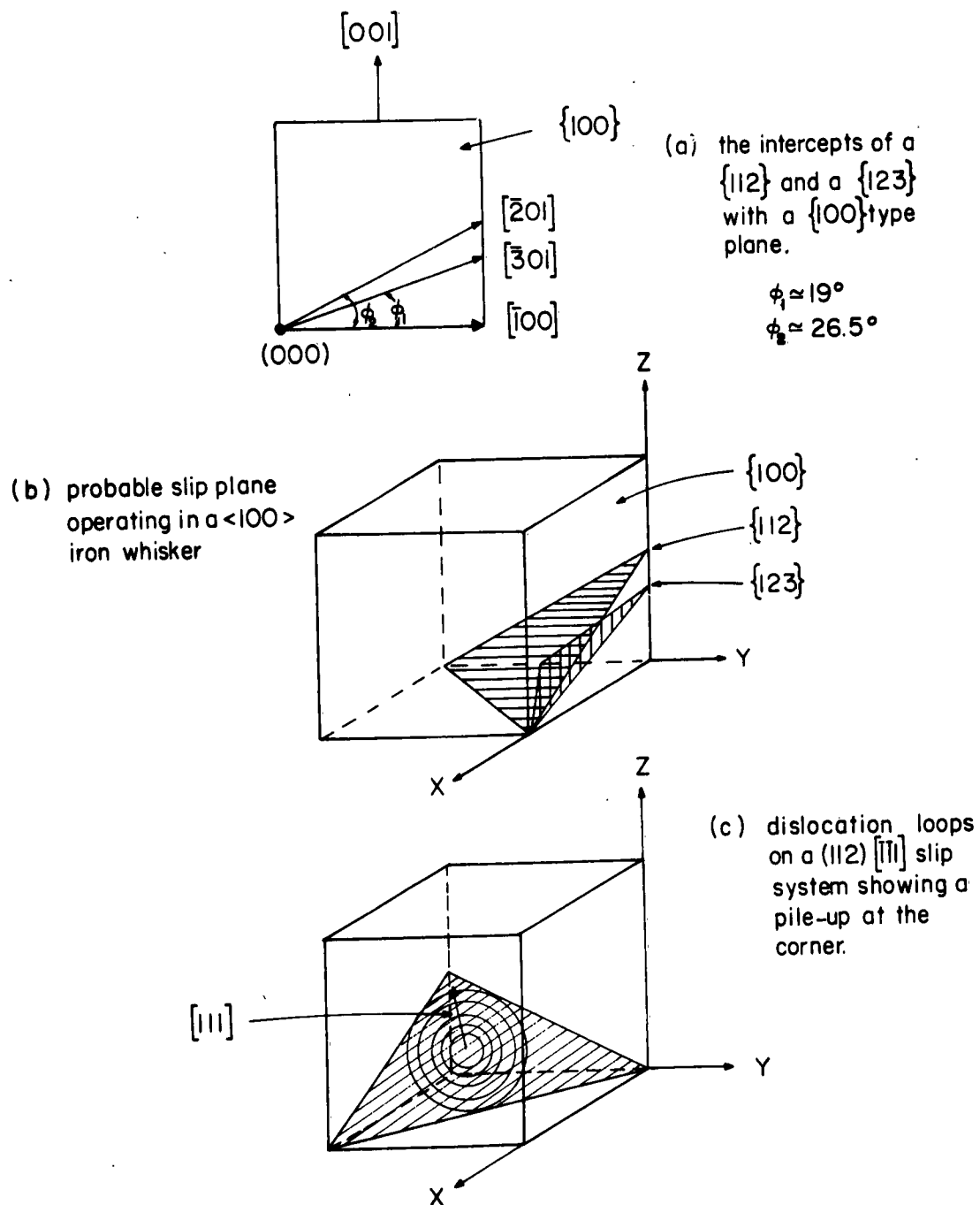


Figure 34

In summary, therefore, it can be reasonably stated that slip had occurred on  $\{112\} < 111 >$  and/or  $\{123\} < 111 >$  slip systems and that the dislocations slipped out except at the corners where they were attacked and a channel was in fact etched. The reliability of aqueous solutions of copper-ammoniacal-chloride to develop etch pits at dislocations sites has been clearly substantiated. The usefulness of this etchant for defect structure studies must be considered, although it is felt that much better etchants can be developed by the use of halide "poisons."

The results obtained using copper-ammoniacal-chloride electrolytically were not nearly so satisfactory as those obtained by immersion. The shapes of the usual size etch pits were generally poor and the density very large. The presence of the very large pits added uncertainty to the results obtained, especially the very irregular, large pits. Finally, the pits observed showed no alignment as was clearly demonstrated by the pits from immersion tests. It can be concluded, however, that lower current densities than suggested by Kehl<sup>33</sup> provide better results, i.e., approximately 0.3 amp/cm<sup>2</sup> instead of 0.5 amp/cm<sup>2</sup>.

The very large, irregular pits, Figs. 10 and 11, most probably resulted from preferential electrochemical attack at anodically active areas. These very active areas were localized occurrences and probably resulted from a superficial origin. The extremely irregular shape of the pits formed at these sites suggests that indeed the attack was catalyzed and an adsorbed impurity most probably was present. A pit resulting from a physical driving force, viz., the strain energy of a dislocation, would develop a regular geometrical shape as dictated by crystallographic symmetry. The fact that these localized sites were electrochemically more active would infer that these were preferred adsorption sites. In any respect, these pits were not the result of a defect structure alone.

#### B. HYDROCHLORIC ACID

The etchants based on hydrochloric acid dissolved in ethanol and poisoned with CuCl<sub>2</sub> have proved successful. The primary limitation of these solutions is the small size of the etch-pits that are formed. That these etchants do in fact develop etch-pits at dislocation sites has been demonstrated by the formation of pits aligned along a tilt boundary. Pits are preferentially formed along tilt-boundaries early and persist throughout subsequent immersion periods.

The usefulness of Cl<sup>-</sup> as a poison has been reported many times in the literature, and for a variety of materials. However, in the case of iron whiskers grown by means of hydrogen reduction of FeCl<sub>2</sub>, the actual origin of the poison is not straightforward. Does the effective poison content come from the CuCl<sub>2</sub> additions or in fact, does it result from a minute chloride residue adsorbed on the whisker surface? Observations of many dissolution experiments indicated that superficial impurities do exert a finite influence in some cases, at least. Attempts to ascertain the optimum conditions of poison concentration, i.e., CuCl<sub>2</sub>, and immersion time based upon this dissolution ledge inhibition reflected the uncontrollable variable

of surface purity. Consequently, the results were ambiguous and concentrations over a wide range, viz.,  $1.1 \times 10^{-4}$  to  $3.7 \times 10^{-6}$  mole-fraction of  $\text{CuCl}_2$ , showed excellent results in some cases, and yet poorer pits were formed in others. In the summary, however, it will suffice to state that the good results were more frequently obtained than the poorer results.

### C. HYDROFLUORIC ACID

In order to circumvent the above complication, attempts were made to use the  $\text{F}^-$  ion as a poison. This ion does in fact satisfy the requirements of a useable poison in that it forms a series of stable complexes with iron. The  $\text{F}^-$  ion has a size that is more comparable to the iron lattice than the  $\text{Cl}^-$  ion and hence in this respect, the fluorine should be superior. However, the over-all performance is surely affected by the ionization of the acid and in this respect,  $\text{HCl}$  is definitely superior. Therefore, it is not at all evident that fluorine can mask the effects of adsorbed  $\text{Cl}^-$ . A series of experiments undertaken using the  $\text{HF-H}_2\text{O-FeF}_3$  system was designed to compare the effective poisoning of  $\text{F}^-$  with respect to  $\text{Cl}^-$ .

The series of tests using solutions of varying concentrations of  $\text{HF}$  in water showed that the dissociation of the  $\text{HF}$  to form  $\text{F}^-$  ion was indeed limited. The dissolution of the iron whiskers was small due to the weak acidity of these solutions and hence the corresponding pit sizes were small, however, comparable to the pit size developed in  $\text{HCl}$  solutions. The effectiveness of the  $\text{F}^-$  ion poison was demonstrated by the fact that concentrations above 10 mole-percent showed no discernable attack, probably due to increased  $\text{F}^-$  concentration.

Figure 17 shows the dissolution rate of iron whiskers as a function of  $\text{HF}$  concentration in aqueous solution. The shape of this curve appears to be very irregular; however, this curve can be explained, qualitatively at least. Figure 35 shows a curve representing the concentration of  $\text{FeF}_3$  at saturation as a function of  $\text{HF}$  concentration. The similarity of these curves is immediately evident and hence it can be concluded that the curve in Fig. 17 signifies the formation of a  $\text{Fe-F}$  complex, most probably  $\text{FeF}_2^{--}$  or  $\text{FeF}_3^{---}$ . These results also demonstrate that  $\text{F}^-$  is effective as a poison and does indeed facilitate etch pit formation. From the results presented in Fig. 17, the 3.0 mole-percent solution was chosen as the base solution for further tests in order to evaluate the effect of  $\text{FeF}_3$  additions. The reason for the selection of this base solution was first, it represented the maximum dissolution rate and second, this concentration was particularly sensitive to changes in  $\text{F}^-$  concentration. Both of these characteristics facilitated the manipulation of dissolution rates in order to preferentially form etch-pits and at the same time, inhibit ledge dissolution laterally.

The results of the additions of the  $\text{FeF}_3$  to the aqueous 3.0 mole-percent  $\text{HF}$  solution, Fig. 19, showed a linear decrease in the dissolution rate with increasing  $\log [\text{FeF}_3 \text{ concentration}]$ . These results are in agreement with the theoretical predictions of Cabrera, (see Appendix IV), who stated that the driving force for dissolution would be proportional to the undersaturation, i.e., the ratio of the actual concentration of dissolving species to the concentration at saturation of this species. The concentration of  $\text{FeF}_3$

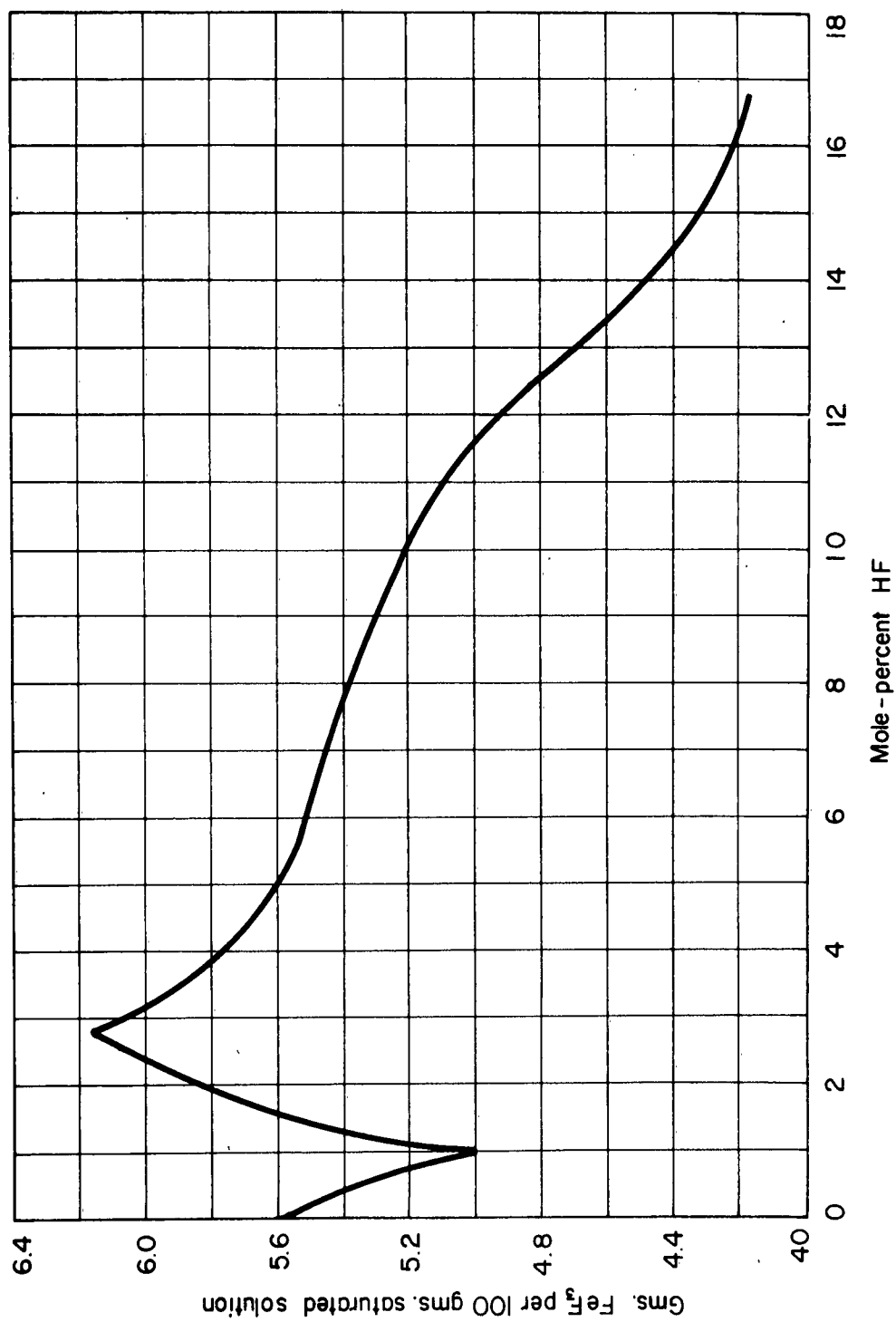


Figure 35: The amount of  $\text{FeF}_3 \cdot 3\text{H}_2\text{O}$  as a function of mole-percent of HF in 100 gms saturated solution in  $\text{H}_2\text{O}$  at  $25^\circ\text{C}$  at equilibrium in the  $\text{HF} - \text{FeF}_3 - \text{H}_2\text{O}$  system.

is in fact proportional to the undersaturation. The equilibria involved in the  $\text{HF-H}_2\text{O-FeF}_3$  system studied have been solved, with the assistance of Messrs. J. F. Lindley and J. O. Reebel, Civil Engineering, Ohio State University, using an IBM 7090 computer. These results will be used to calculate the actual undersaturation values and the dissolution rates will then be plotted as a function of undersaturation. Such a graph would be more meaningful in ascertaining if Cabrera's postulates hold for the dissolution of iron whiskers under the conditions imposed.

The significance of these studies is that if Cabrera's statements do in fact obtain, judicious manipulation of the undersaturation would result in etch-pit formation at defect sites and reliably only at defect sites. Undersaturations could be used such that dissolution would be energetically unfavorable on a perfect surface; only at defect sites, where an additional driving force, viz., strain energy, is present could dissolution occur. This would result in dislocation etch-pits being formed preferentially.

The errors involved in the above studies originated primarily from two sources: (1) the chemical analyses and (2) the measurement of surface areas. The dissolution rates were determined by measuring the iron pick-up in the etchant and relating this to the surface area. The technique employed was a colorimetric procedure in which the  $\text{Fe}^{+++}$  ion color was developed by means of 1,10-phenanthroline and the resulting transmittancy measured against a suitable blank using a Coleman Spectrophotometer.

Careful preparation of the blanks and accurate calibration of the spectrophotometer eliminated any major sources of error in the procedure. Also, cross-checking against known standards assured consistency in the analyses. Contamination was the most obvious source of error but the use of blanks compensated for these sources. Possible failures in the procedure, such as incomplete dissolution of the iron-fluorine complexes, the presence of impurities such as  $\text{F}^-$  which could reduce the  $\text{Fe}^{+++}$  color, etc., were all realized and proper precautions were taken. There were inherent errors involved in the equipment used, i.e., balances and volumetric equipment. The latter did in fact limit the concentration of  $\text{FeF}_3$  which could be accurately handled because the magnitude of dilution required in order to bring the iron concentration into the range of the spectrophotometer was too great and the error too large. The maximum error to be expected in the chemical analyses should not exceed  $\pm 5\%$ .

By far, the most significant source of error was the measurement of surface areas. This was accomplished under the microscope, using magnifications up to 500X. The effective volume of iron dissolved away was measured and the depth of attack determined by dividing this volume by the surface area. The original area was used in these calculations; however, it is known that this area does indeed change as dissolution proceeds. Therefore, the error inherent to these calculations was determined, (see Appendix V). The errors involved were found to be as follows:

< 100 > whiskers	~ 10%
< 111 > whiskers	~ 6%.

These errors are probably smaller than the errors inherent to the dimensional measurements and so the method used in the calculation of dissolution rate was acceptable. Also, there is no reason to expect the whiskers to be truly regular and the idealized treatments used in the calculations of area change are limited in scope and applicability. The total error to be expected would therefore be of the order of approximately  $\pm 10\%$ .

The work done using  $H_2SO_4$  solutions containing  $K_2S_2O_8$  suggested certain requirements necessary for the formation of large, well-defined etch-pits in iron whiskers.

#### 1. Presence of an Internal Poison

The abrupt change in the shape of etch-pits observed in different layers of the whisker was attributed to a variation in the amount of internal poison present. Most whiskers had one concentration of poison in the shell and another in the core. While this was shown in almost all the whiskers, it is particularly striking in Figs. 26 and 27. Well-shaped pits were present in the shell and shallow pits in the core. As-grown dislocations were present in both shell and core. Since the etchant in both cases was the same, the poison must have been contained within the whisker. A considerably higher concentration of poison was present within the shell than apparently was present in the core. Poisons, when added to the etchant, operate by adsorbing on the advancing ledges. It has been assumed that an internal poison dissolves, builds up in the solution adjacent to the crystal, and adsorbs on the ledges in a similar manner. The effect of the poison was apparently quite localized, since the poison in the shell retarded only pits formed in the shell. The poison also affected deformation dislocations, indicating that segregation of poison along the dislocation line was not required.

Since as-grown dislocations were present in the core as well as the shell, it is felt that the final thickness of a whisker results primarily from the nucleation and growth of side ledges rather than from a single axial screw dislocation. The poison concentration probably builds up on the sides of the whisker during thickening. When the concentration on the surface reaches a certain level, the poison is incorporated into the lattice at a faster rate. This marks the shell-core interface. Wiedersich,<sup>39</sup> shows that an equilibrium existed between gaseous  $H_2$ ,  $HCl$ , and  $FeCl_2$ , and the solid  $FeCl_2$  and  $Fe$  during growth of the whiskers. Adsorbed  $FeCl_2$  and  $HCl$  molecules were present on a whisker during growth and could easily be incorporated into the whisker lattice. Since it has already been shown that halide ions act as poisons when present as additions to the solution, it is very likely that they could also act as an internally contained poison. It was therefore postulated that chlorine in some form was acting as the internal poison, although the amounts of chlorine present were not sufficient to be determined quantitatively.

#### 2. Length of Dislocation Line

Besides having a favorable poison concentration and dissolution rate, large etch pits formed only if the dislocation line was sufficiently

long. In this work the dislocation lines terminated at the shell-core interface, so that the pits could not become deeper than the shell thickness.

### 3. Correspondence of Etch Pits and Dislocation Sites

The results indicated that the internal factors of the whisker determined to a large degree whether pits were observable. In the cases where well-resolved etch pits formed, the correlation between etch pits and dislocations was probably good. The etchants were generally found not to produce equally well-defined pits on both {100} and {110} whisker faces.

The 1N  $H_2SO_4$  + 0.2N  $K_2S_2O_8$  etchant was ideally suited for the etching of {100} faces of both rectangular and square whiskers. Sharp-bottomed pits, such as shown in Fig. 21, resulted from attack along a line defect, strongly suggesting dislocation attack. The density of the large pits remained constant with time, as must be the case for pits at as-grown dislocation sites. When the pits were small and the density high, this was more difficult to determine, but the number appeared to remain constant. The existence of a shell and core on most whiskers prevented the number of pits from remaining constant over extended etching periods. The underlying core often had a completely different dislocation density and internal poison concentration. The 1N  $H_2SO_4$  + 0.2N  $K_2S_2O_8$  etchant normally developed observable etch pits in the core of square and rectangular whisker, although these pits were usually shallow because of a lower poison concentration in the core. When the poison content of the core was very low, neither as-grown nor deformation-produced dislocations would etch as well-defined pits, Fig. 27.

The 1N  $H_2SO_4$  + 0.2N  $K_2S_2O_8$  etchant was less satisfactory for etching hexagonal whiskers. The agreement of dislocations and etch pits was probably good in the shell, but the pits were less clearly defined. On {110} planes in the core where the poison content was usually lower, this environment was unsatisfactory for revealing as-grown dislocations.

Figures 21b, 26b, and 28 show that the pit density increased markedly after deformation as must be required by the increased dislocation density. Based on the above consistencies, it is felt that the 1N  $H_2SO_4$  + 0.2N  $K_2S_2O_8$  etchant produces pits only at dislocation sites. In unfavorable conditions of orientation and internal poison concentration, no etch pits were observed. There was no indication, however, that etch pits formed at sites other than where dislocations intersected the surface.

The picral and nital were used to etch only undeformed whiskers. The picral etch was usually found unsuitable for revealing as-grown dislocations on {100} faces, even in the shell where the poison content was higher. The 4% picral solution produced well-defined etch pits in the shell of hexagonal whiskers. The etch pits observed after several minutes of etching most probably were located at dislocation sites, Fig. 29a. With extended etching, considerable background attack was observed, Fig. 29b, which was probably not associated with dislocations. On {110} planes in the core of hexagonal whiskers where the poison was lower, 4% picral was unsatisfactory for revealing dislocation sites, Fig. 31c.

Etch pits produced on hexagonal whiskers after several minutes of etching in 2% nital probably agreed well with the dislocations present, Fig. 30a. Background attack which resulted after etching for 10 min. was very likely not associated with dislocations, Fig. 30b. The 2% nital was the only etchant suitable for revealing as-grown dislocations on {110} planes in the core of hexagonal whiskers, Fig. 31d. Since the core was etched in the nital for only 3 min., it is felt that these pits do represent as-grown dislocation sites. Pits formed after a short etch in nital probably represented dislocation sites. The creation of {110} faces on the corners of square whiskers often removed the original {110} faces before etch pits on the {100} faces could be formed.

The dissolution rate, length of the dislocation line, and poison concentration all influence the formation of well-shaped etch pits. The environment establishes the dissolution rate. In the case of iron whiskers, the poison was present internally and must have been present at a high enough concentration or none of the etchants discussed here would have produced satisfactory etch pits.

#### 4. Dislocation Structure of Whiskers

Nearly all whiskers appeared to have a distinct shell and core region. The as-grown dislocation density in these two regions usually was considerably different. Symmetric etch pits at as-grown dislocations in the shell indicated that these dislocations intersect perpendicularly to the surface. The as-grown dislocations in the core of square and rectangular whiskers were probably also aligned perpendicularly to the surface. The alignment of as-grown dislocations in the core of a hexagonal whisker was probably more complex. The perpendicular alignment of the dislocations undoubtedly arose because of image forces present during and after crystal growth.

The as-grown dislocations in the shell probably were attached to some type of two-dimensional dislocation network along the shell-core interface, very likely at nodes formed where two or more dislocation lines lying along the interface intersected each other. Since this network lay parallel to the reference surface, it could not be observed during etching. The fact that the shell and core did not always have the same orientation supports the idea of a dislocation network at the shell-core interface.

The number of as-grown dislocations in the core, which were attached to nodes at the shell-core dislocation network, bore no relationship to the number of dislocations in the shell attached to nodes from the other side. The dislocation density in the shell can be greater or less than that found in the core. Less is known about the dislocations in the core because pits with crystallographic shape usually did not etch at these dislocations. Except for the poison concentration, which was often less, these dislocations were probably similar to those in the shell.

The dissolution rates determined using the  $\text{H}_2\text{SO}_4 + 0.2\text{N K}_2\text{S}_2\text{O}_8$  were calculated somewhat differently from those previously discussed. The two



methods for determining dissolution rate were by the change in cross sectional shape during etching and again by analyzing the solution for iron pick-up. Both methods were used to determine the rate of dissolution perpendicular to the {100} face of one large square and one large rectangular whisker supplied by C. M. Wayman. The thickness of the as-grown whiskers was measured and the whiskers then etched in  $1N H_2SO_4 + 0.2N K_2S_2O_8$ . The etched whiskers were then cross sectioned and the change in thickness was measured.

Approximately  $33\mu$  were removed perpendicular to each {100} face of the rectangular whisker in 1 hr. 40 min. This corresponded to a rate of penetration of  $0.33\mu/min$ . Applying Faraday's law, it was found that this in turn corresponded to a corrosion current density of approximately  $15ma/cm^2$ . In a similar manner,  $7.5\mu$  were removed perpendicular to each {100} face of the square whisker in 25 minutes. This corresponded to a corrosion rate of  $14ma/cm^2$ .

Figures 36; 37, and 38 show the polarization behavior of alpha iron single crystals as determined by Engell. Figure 38 shows the polarization resulting from a  $1N H_2SO_4 + 0.5N (NH_4)_2S_2O_8$  solution, using a pure iron anode.  $I_{Fe+2}$  represents the rate of dissolution of iron calculated on the basis of the apparent surface area from the iron content in the solution and Faraday's law.  $I_c$  represents the curve of the externally applied cathodic current density versus potential.  $I_{ox}$  shows the polarization curve for the cathodic half reaction, which in this case is the reduction of persulfate to persulfite.

Figure 38 shows that a corrosion rate of  $15ma/cm^2$  on a {100} face corresponds to a corrosion potential of  $-164$  mv SHE or  $-406$  mv SCE. The measurement of the single electrode potential of an iron whisker corroding in  $1N H_2SO_4 + 0.2N K_2S_2O_8$  should indicate how closely the dissolution rate of the whiskers agrees with the results found for large iron single crystals.

Figure 42 shows the potential time graphs for these whiskers. It can be seen that the corrosion rate calculated from the change in cross section perpendicular to the {100} face agrees very well with the corrosion rate corresponding to the measured potential as obtained from Fig. 38  $SCE(mv) + 242$  mv = SHE(mv).

The solutions described in Fig. 42 were analyzed for their iron content after the measurement of potential. Based on the iron analysis, the rectangular had a corrosion rate of  $21 ma/cm^2$  while the square whisker had a corrosion rate of  $39 ma/cm^2$ . A somewhat higher dissolution rate was expected because the dissolution of the corners creates higher order planes which dissolve at a faster rate. Some error in the measurement of surface area might also have occurred. Even taking the above possibilities into account, the dissolution rate calculated from the iron content in solution was higher than expected, especially the  $39 ma/cm^2$  calculated for the square whisker. The etch pits on both of these whiskers were shallow. The calculation of corrosion rates as described above cannot be applied directly to a surface containing large, well-developed pits.

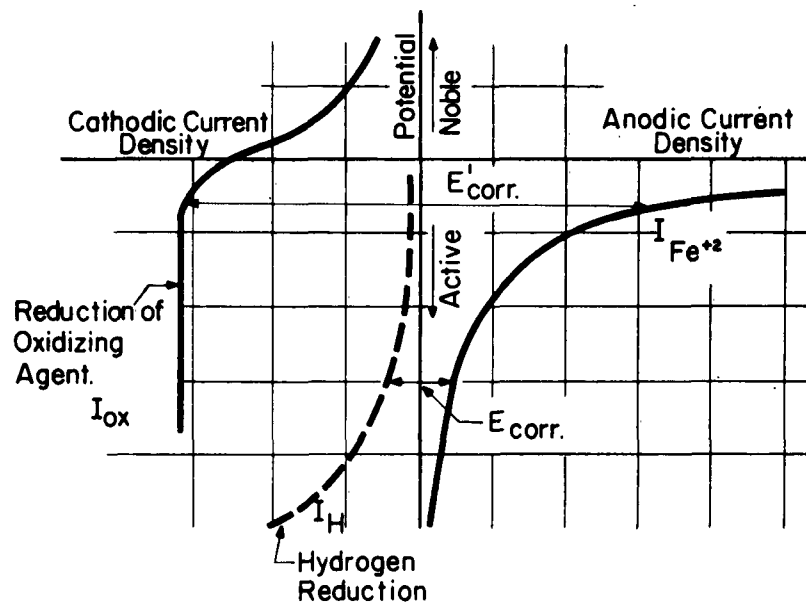


Figure 36: Influence of an oxidizing agent on the polarization curves for the corrosion of iron in acids

$E_{corr}$  = Corrosion potential of iron in acid

$E'_{corr}$  = Corrosion potential of iron in acid with an oxidizing agent added

$I_{Fe^{+2}}$  = Rate of corrosion of iron found by analysing the solution

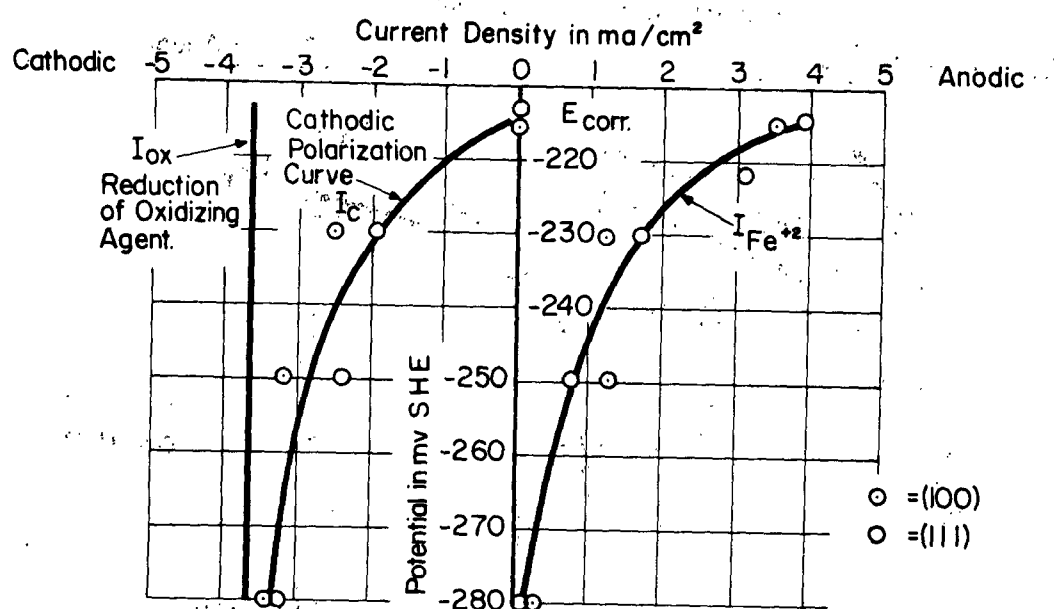


Figure 37: Polarization behavior of iron in 1N  $H_2SO_4$  + 0.02N  $K_2S_2O_8$ .

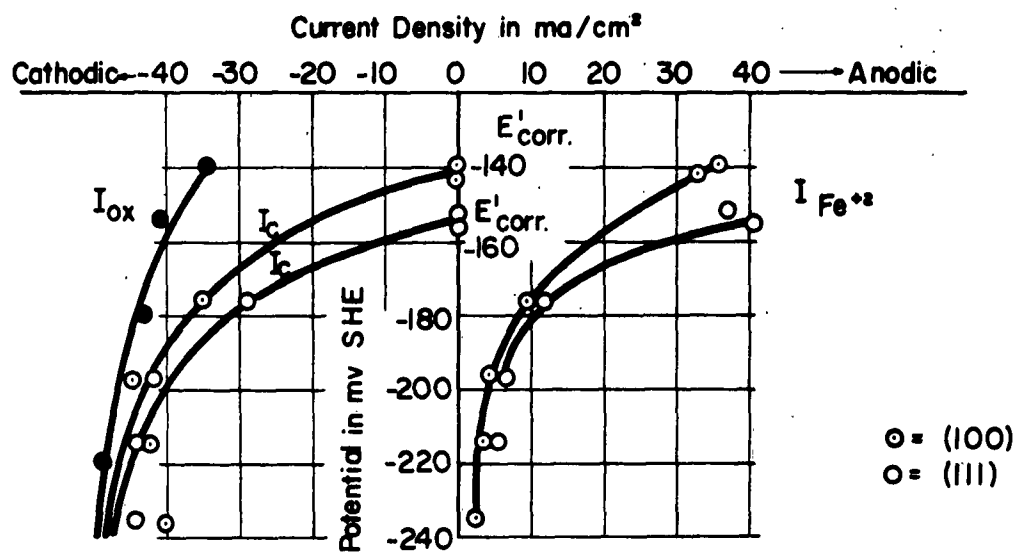
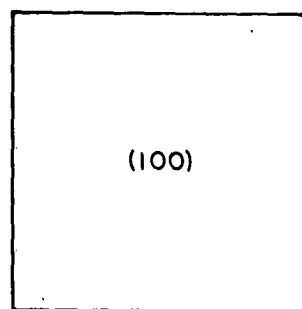
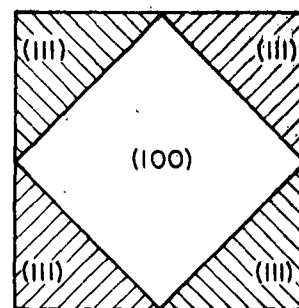


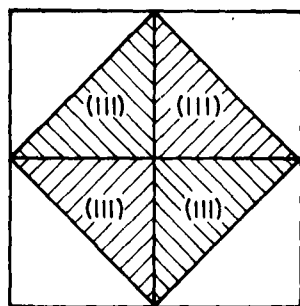
Figure 38: Polarization behavior of iron in 1N  $\text{H}_2\text{SO}_4$  + 0.5N  $(\text{NH}_4)_2\text{S}_2\text{O}_8$ .



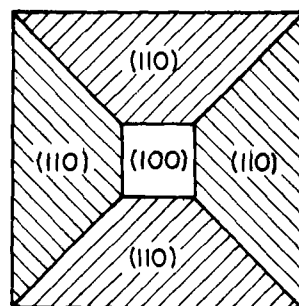
a  
Five (100) Planes



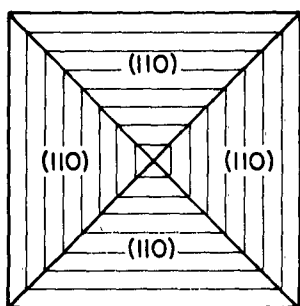
b  
(100) Bottom, (111) Sides



c  
(111) Sides

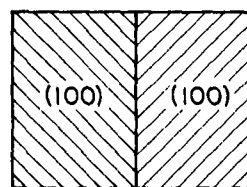


d  
(100) Bottom, (110) Sides



e  
(110) Sides

(110) Projection



f  
Rectangular  
Pit with (100)  
Sides.

Figure 39: Schematic Representation of Etch Pits as Projected on (100) and (110) faces, a through e are (100) projections.

## 5. Determination of the Preferred Slip Planes

Figure 40a shows the most probable slip systems operating during the deformation of whiskers of each of the three growth directions. The formation of etch pits at newly created deformation-produced dislocations does not in itself indicate the slip plane, since the density of pits was usually too high, and the pits usually were randomly scattered.

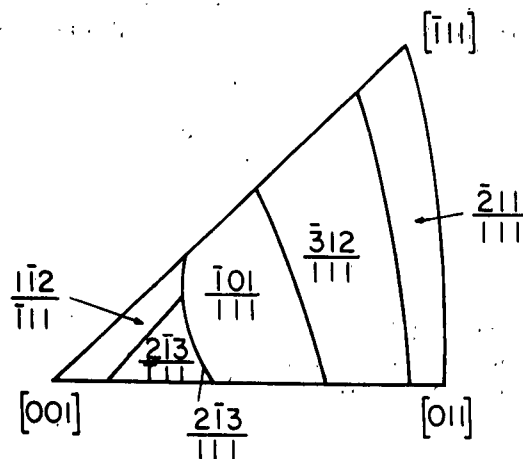
While most of the whiskers when deformed did not produce slip lines on the surface, one square and one rectangular whisker did show slip lines after deformation. The slip system(s) causing these slip lines can be determined from a consideration of the most probable slip systems based on the critical resolved shear stress. Based on the conventions in Fig. 40a, the  $(1\bar{1}2)[\bar{1}11]$  or  $(2\bar{1}3)[\bar{1}11]$  are the most probable slip systems for a  $\langle 001 \rangle$  whisker.

The angles of intersection of these slip systems with a  $\langle 001 \rangle$  whisker axis are shown in Fig. 41a. Figure 41c and 41d show the theoretical angles of intersection of the  $(1\bar{1}2)$  and  $(2\bar{1}3)$  planes with the  $\{100\}$  whisker surface. The angle of  $62^\circ$  found experimentally agrees very closely with the angle of  $63.4^\circ$  for the  $(1\bar{1}2)$ , while  $70^\circ$  agrees very well with  $71.6^\circ$  for a  $(2\bar{1}3)$  plane. The operating slip systems are indeed those predicted from Fig. 40a.

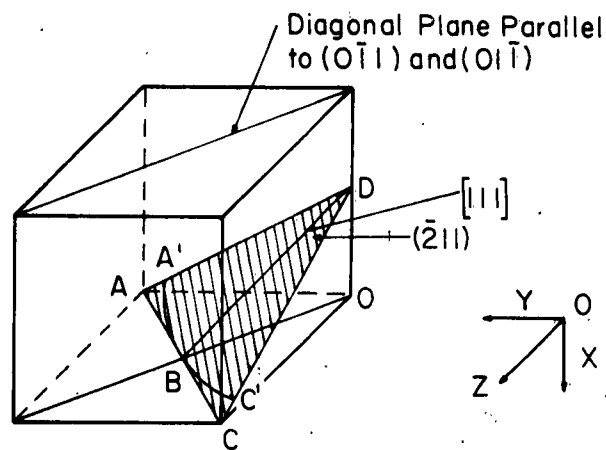
Slip lines observed on a  $\{100\}$  face of a rectangular whisker also appear to belong to two slip systems, one with positive slope and one with negative slope. The angles measured from photomicrographs are shown in Fig. 41b. Figure 41c shows the theoretical angles of intersection of the  $(\bar{2}11)$  and  $(\bar{3}12)$  slip planes, which are favored for a  $[011]$  whisker axis. The angles observed do not agree with either of these slip systems. These angles agree with the slip systems  $(1\bar{1}2)[\bar{1}11]$  and  $(2\bar{1}3)[\bar{1}11]$ , however, assuming a  $[001]$  rather than a  $[011]$  growth axis. It is felt that this was probably another example of a whisker in which the shell and the core did not have the same orientation. The rectangular shape probably resulted from a  $[011]$  growth axis of the core. The very thin shell over this core was apparently a  $\{100\}$  face but rotated  $45^\circ$  into a  $[001]$  orientation.

## 6. Rotation of the Shell and the Core

One example of the rotation of the shell and the core was provided in the previous section. This rotation was observed on at least two other rectangular whiskers by the orientation of the etch pits. Since the  $1N H_2SO_4 + 0.2N K_2S_2O_8$  etchant preferentially forms pits on  $\{100\}$  planes delineated by  $\{110\}$  side faces, the orientation of the pits can be used to determine the growth axis of the whisker. Figure 39 shows schematically the shape of etch-pits commonly observed and from these etch-pits, the whisker orientation can be determined. Using these techniques, rotations in shell and core have been measured.



(a) Regions of a unit triangle within which the indicated resolved shear stresses in a bcc lattice is higher than other resolved shear stresses



(b) Intersection of slip plane  $(\bar{2}11)$  with whisker faces  $(0\bar{1}1)$  and  $(01\bar{1})$

Figure 40

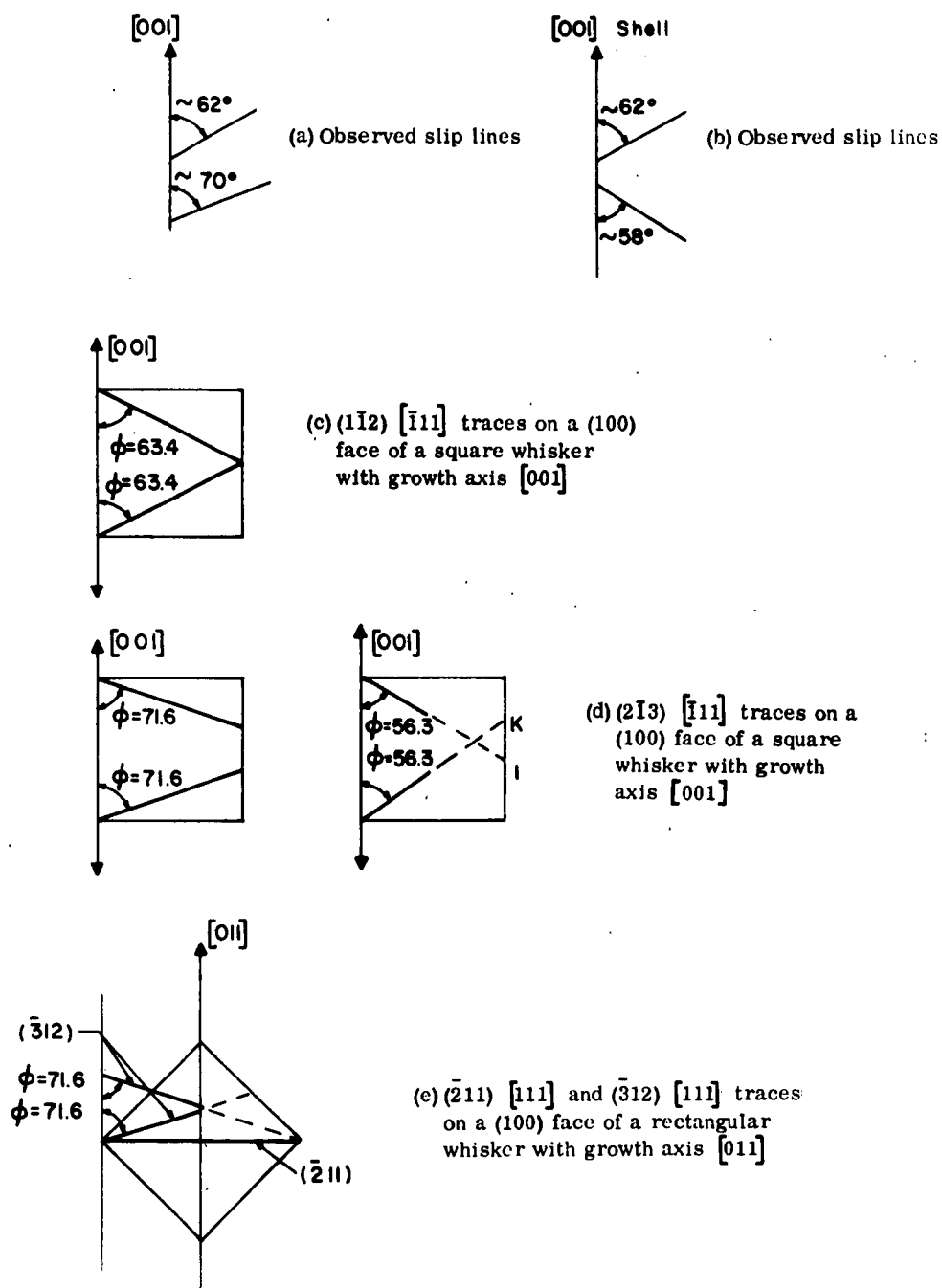
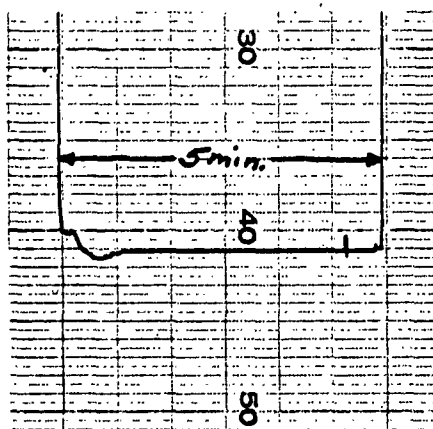
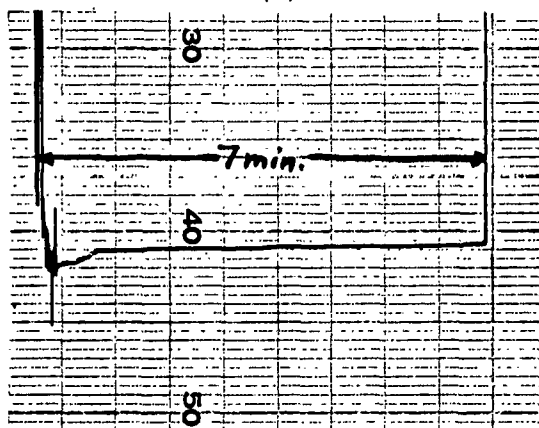


Figure 41: Traces of slip systems on whisker faces





(a)



(b)

Figure 42. Potential time traces in 1N  $H_2SO_4$  + 0.2N  $K_2S_2O_8$   
a) Rectangular whisker  
b) Square whisker

The initial instability in (b) resulted from a loose connection in the measuring circuit.  
30, 40, 50 correspond to -300, -400, -500 millivolts active to the saturated calomel electrode (SCE).

## V. CONCLUSIONS

1. Most whiskers were composed of a distinct shell or overgrowth surrounding the core. This shell ranged in thickness from less than one micron up to several microns. The as-grown dislocation density in the shell can be either greater or less than in the core. The as-grown dislocations were thought to be attached to nodes formed by a two-dimensional dislocation network parallel to the surface at the shell-core interface.

2. The shell and core did not always have the same orientation. On the (100) face of three rectangular whiskers, the shell was rotated  $45^\circ$  with respect to the core. The shell had a [100] growth axis while the core was [110].

3. Etch pits at as-grown dislocations were symmetric indicating that the dislocations were perpendicular to the surface. The etch pits at clean deformation-produced dislocations formed asymmetric pits whenever the pits were large enough to discern their shape.

4. Three requirements were established for the formation of large well-defined etch pits in iron whiskers: a) presence of an internal poison-- etch pits present in the shell were usually smaller and better-contained than pits in the whisker core. This abrupt variation in the shape of pits in different layers of the whisker, even though etched in the same solution, has been attributed to a change in the concentration of an internal poison. In a layer with a high poison concentration, well-defined pits were formed at both clean deformation-produced dislocations and at as-grown dislocations. In a layer with a low poison concentration, pits at both types of dislocations were wide and shallow, b) dissolution rate -- better-defined pits were created when the dissolution rate favored pits bound by planes other than the plane of the reference surface. The etchant  $1N H_2SO_4 + 0.2N K_2S_2O_8$  produced better-contained pits on (100) faces than the 4% picral or 2% nital, while on (110) faces the picral and nital etches produced better-defined pits. The  $1N H_2SO_4 + 0.2N K_2S_2O_8$  etch produced pits on (100) faces bound by (110) side faces and having a (100) bottom. The picral and nital etches produced rectangular pits on (110) planes bound by two (100) faces, c) length of dislocation line -- besides a favorable poison concentration and dissolution rate, large etch pits can form only if the dislocation line is sufficiently long. A pit cannot become deeper than the thickness of the shell.

5. Two percent copper-ammoniacal-chloride solutions produced well-defined etch pits upon immersion; however, these pits were very small in size. This etchant does in fact outline the operative slip planes, as was demonstrated using deformed whiskers. The use of this environment is limited because of the copper which plates out of solution onto the iron surfaces. The results obtained using a 0.5% copper-ammoniacal-chloride solution electrolytically were not nearly so satisfactory as those obtained by immersion. The shapes of the etch pits were generally poorer and the density very large. Lower current densities, i.e.,  $0.3 \text{ amp/cm}^2$  as compared to  $0.5 \text{ amp/cm}^2$ , seemed to give better results.

6. The pits formed using a modification of Fry's reagent (HCl + alcohol) which contained  $\text{CuCl}_2$  showed very good, geometrical shapes. These pits, although small, preferentially developed along tilt boundaries in some cases. A solution containing  $3.7 \times 10^{-5}$  mole fraction of  $\text{CuCl}_2$  produced good pits for immersion periods of 10 seconds. These etchants again demonstrated the reliability of  $\text{Cl}^-$  to poison dissolution ledges in order to contain etch pits.

7. Small, but generally well-shaped pits were formed using aqueous solutions of HF. Concentrations greater than 10 mole-percent HF showed only negligible attack on the iron whisker. The addition of  $\text{FeF}_3$  decreased the dissolution rate of iron whiskers in aqueous HF, indicating the effectiveness of  $\text{F}^-$  as a poison. The dissolution rates decreased linearly with increasing  $\log [\text{FeF}_3]$ , which is in fact proportional to the undersaturation.

8. Etchants containing halide ion poisons (viz.,  $\text{F}^-$  and  $\text{Cl}^-$ ) were generally successful in developing well-defined etch pits.

# REFERENCES

1. Coleman, R. V., J. Appl. Phys., 29, 1487 (1958).
2. Coleman, R. V., in Growth and Perfection of Crystals (John Wiley and Sons, Inc., New York, 1958), p. 239.
3. Wayman, C. M., J. Appl. Phys., 32, 1844 (1961).
4. Brenner, S. S., J. Appl. Phys., 27, 1484 (1956).
5. Rambauske, W. R., and R. R. Gruenzel, X-ray Diffraction Investigation on Iron Whiskers, Technical Documentary Report No. ASD-TDR-62-331 (1962).
6. Gorsuch, P. D., and T. H. Alden, Research on the Behavior of Nearly Perfect Crystals, Final Report, Contract No. AF 33(616)-6181 (1961).
7. Liss, R. B., Acta. Met., 7, 231 (1959).
8. Boswell, F. W. C., Metal Progress 72, 92, December (1957).
9. Smith, Dana W. and Robert F. Mehl, Metals and Alloys, 4, 31 (1933).
10. Svetchnikoff, M. V. N., Revue de Metallurgie, 27, 404 (1930).
11. Young, F. W. Jr., J. Appl. Phys., 32, 192 (1961).
12. Mendelson, S., J. Appl. Phys., 32, 1579 (1961).
13. Cabrera, N., in Semiconductor Surface Physics, (University of Pennsylvania Press, Philadelphia, 1957), p. 327.
14. Frank, F. C., in Growth and Perfection of Crystals (John Wiley and Sons, Inc., New York, 1958), p. 411.
15. Lovell, L. C., and J. H. Wernick, J. Appl. Phys., 30, 590 (1959).
16. Livingston, J. D., J. Appl. Phys., 31, 1071 (1960).
17. Rosenbaum, H. S., and M. M. Saffren, J. Appl. Phys., 32, 1866 (1961).
18. Gilman, J. J., W. G. Johnston, and G. W. Sears, J. Appl. Phys., 29, 747 (1958).
19. Berlec, I., J. Appl. Phys., 33, 197 (1962).
20. Gilman, J. J., and W. G. Johnston, "Dislocations and Mechanical Properties of Crystals," 1956 Lake Placid Conference (John Wiley and Sons, Inc., New York, 1957) p. 116.
21. Young, F. W. Jr., J. Appl. Phys., 29, 760 (1958).

22. Gilman, J. J., Trans. AIME, 206, 998 (1956).
23. Hibbard, W. R., and C. G. Dunn, Acta. Met., 4, 30C (1956).
24. Amelinckx, S., Phil. Mag., 1, 269 (1956).
25. Holmes, P. J., Acta. Met., 7, 283 (1959).
26. Gilman, J. J., Trans. AIME, 212, 310 (1958).
27. Johnston, W. G., in "Progress in Ceramic Science," Vol. 2, (Pergamon Press, New York).
28. Cabrera, N., and D. A. Vermilyea, in "Growth and Perfection of Crystals," (John Wiley and Sons, Inc., New York, 1958) pp. 393-408.
29. Batterman, B. W., J. Appl. Phys., 28, 1236 (1957).
30. Engell, H. J., Arch. Eisenhüttenw., 26, 393 (1955).
31. Handbook of Chemistry and Physics; 40th ed., p. 1650 (1958).
32. Befglund, Torkel; Metallographer's Handbook of Etching, London, Sir Isaac Pitman and Sons, Ltd. (1931).
33. Kehl, George L., Principles of Metallographic Laboratory Practice, McGraw-Hill Book Co., Inc., New York, p. 433-43-45 (1949).
34. Sears, Gerald W., J. Chem. Phys., 32, 1317 (1960).
35. Weik, H., J. Appl. Phys., 30, 789 (1959).
36. Opinsky, A., and R. Smoluchowski, Carnegie Institute of Technology Symposium on the Plastic Deformation of Crystalline Solids, Office of Naval Research, 1950, p. 216.
37. Cullity, B. D., Elements of X-ray Diffraction, Addison-Wesley Publishing Co. Inc., Reading, Mass., 72, (1956).
38. Barrett, C. S., Structures of Metals, McGraw-Hill Book Co. Inc., New York (1952).
39. Wiedersich, H., J. Electrochem. Soc., 106, 810, (1959).

# APPENDIX

(I) Calculation of tilt-boundary angle from etch-pit spacing:

$$\tan \theta = b/d$$

where

b = Burger's vector

d = separation

$$\bar{b} = a/2 < 111 >$$

$$b = \frac{\sqrt{3}}{2} (2.86 \times 10^{-8} \text{ cm}) = 2.48 \times 10^{-8} \text{ cm}$$

$$d_{(\text{avg.})} \sim 1 \times 10^{-3} \text{ cm}$$

$$\tan \theta \simeq \frac{2.48 \times 10^{-8}}{1 \times 10^{-3}} \simeq 2.5 \times 10^{-5} \text{ radians}$$

$$\tan \theta \simeq 1.4 \times 10^{-3} \text{ degrees}$$

(II) Calculation of dissolution rate:

Immersion period was 60 seconds. Used a 25 ml sample for these analyses.

Transmittancy of etchant compared to the blank = 90.8%.

From calibration curve: 90.8% = 0.023 mg  $\text{Fe}_2\text{O}_3$  per 100 ml

$$\text{Fe pick-up} = (0.023)\left(\frac{1}{4}\right)\left(\frac{111.70}{159.70}\right) = 0.004 \text{ mg Fe.}$$

$$\text{Surface area of whisker} = 1.8 \times 10^{-3} \text{ cm}^2.$$

$$\text{Dissolution rate} = \frac{0.004 \times 10^{-3} \text{ gm}}{7.86 \text{ gm/cm}^3} \times \frac{1}{1.8 \times 10^{-3} \text{ cm}^2} \times 10^4 \text{ } \mu/\text{cm}.$$

$$\text{Dissolution rate} = 2.9 \text{ } \mu/\text{min.}$$

(III) Calculation of angle of intersection between two planes in a cubic crystal:

Intersecting planes are the  $(\bar{3}01)$  and the  $(100)$ :

then

$$\cos \phi = \frac{h_1 h_2 + k_1 k_2 + l_1 l_2}{\sqrt{h_1^2 + k_1^2 + l_1^2} \cdot \sqrt{h_2^2 + k_2^2 + l_2^2}}$$

$$\cos \phi_{(\bar{3}01)(100)} = \frac{\bar{3} + 0 + 0}{\sqrt{9+0+1} \cdot \sqrt{1+0+0}} = .946$$

$$\cos \phi_{(\bar{3}01)(100)} \approx 19^\circ$$

$$\cos \phi_{(201)(100)} = \frac{2 + 0 + 0}{\sqrt{4+0+1} \cdot \sqrt{1+0+0}} = .895$$

$$\cos \phi_{(201)(100)} \approx 26\frac{1}{2}^\circ$$

(IV) Calculation of undersaturation:

Note: this derivation was based on disc-shaped vacancies formed in the substrate lattice

$$\alpha = \text{undersaturation} = \frac{(\text{concentration})}{(\text{concentration})_{\text{saturated}}}$$

$$\alpha = \exp - \frac{\pi h \gamma^2 M}{\rho R T^2 \ln B}$$

where: B = a frequency factor for the nucleation,  $\ln B \sim 4-6$  (based on vapor-solid systems)

h = height of vacancy (cm)

$\gamma$  = surface energy  $\left( \frac{\text{ergs}}{\text{cm}^2} \right)$

$\Omega = M/\rho$  = mol volume ( $\text{cm}^3/\text{mole}$ )

R =  $9.3166 \times 10^7 \left( \frac{\text{ergs}}{\text{mole} \cdot \text{deg}} \right)$

k =  $1.38047 \times 10^{-16} \left( \frac{\text{ergs}}{\text{deg}} \right)$

T = temperature ( $^{\circ}\text{K}$ )

$$h_{(100)} = 1.43 \times 10^{-8} \text{ cm}$$

$$h_{(110)} = 2.03 \times 10^{-8} \text{ cm}$$

$$\alpha_{(100)} = \exp - \frac{(3.14)(1.43 \times 10^{-8})(55.85) \gamma_{(100)}^2}{(7.87)(8.32 \times 10^{-7})(1.38 \times 10^{-16})(300)^2(46)}$$

$$\alpha_{(100)} = e^{-(6.69 \times 10^{-8} \gamma_{100}^2)}$$

$$\alpha_{(110)} = \exp - \frac{(3.14)(2.03 \times 10^{-8})(55.85) \gamma_{(110)}^2}{(7.87)(8.32 \times 10^{-7})(1.38 \times 10^{-16})(300)^2(46)}$$



$$\alpha_{(110)} = e^{-(9.50 \times 10^{-6} \gamma_{110}^2)}$$

The dissolution rate is proportional to the undersaturation which in turn depends greatly upon the surface energies. The surface energies are expected to be a function of the crystallographic orientation; based upon 1st and 2nd nearest neighbor bonding approximations  $\gamma_{100} > \gamma_{110}$ .

(V) Change in surface area upon dissolution:

1. The original surface area was assumed to be only negligibly altered, and this original area ( $A^0$ ) was used to calculate the depth of penetration

$$d = \frac{\text{Vol. removed}}{A^0}$$

Now assuming uniform shape and equal penetration around the periphery the actual depth of removal can be calculated:

let:  $\ell$  = length of whisker

$\dot{R}$  = dissolution rate

$t$  = immersion time

$A^0$  = original cross-sectional area

$$A' = \frac{\text{Vol. removed}}{\ell}$$

$A = (A^0 - A')$ , the actual cross-sectional area after immersion

- (a) For  $\langle 100 \rangle$  whiskers:  $x$  = face width after etching  
 $x^0$  = original face width

$$x^2 = A$$

$$x = \sqrt{A}$$

$$\dot{R} = \frac{(x^0/2 - x/2)}{t}$$

$$\dot{R} = \frac{(x^0 - \sqrt{A})}{2t} \quad \text{actual dissolution rate in terms of measurable parameters}$$

- (b) For  $\langle 111 \rangle$  whiskers:  $x$  = face width  
 $h = \frac{1}{2}$  distance between opposite faces

$$h = \frac{x\sqrt{3}}{2}$$

$$A = 2\sqrt{3} h^2$$

$$\dot{R} = \left( \frac{h^0 - h}{t} \right)$$

$$\dot{R} = \frac{1}{t} \left( \frac{x^0\sqrt{3}}{2} - \sqrt{\frac{A}{2\sqrt{3}}} \right)$$

- (c) For  $\langle 110 \rangle$  whiskers:  $a$  = width of  $\{100\}$  face  
 $b$  = width of  $\{110\}$  face

Assuming here that the corrosion depth is not uniform and that instead the shape remains constant, viz.,  $a = \sqrt{2}b$ .

$$a \cdot b = A$$

$$\frac{a^2}{\sqrt{2}} = A$$

$$\dot{R} = \frac{\left( \frac{a^0}{\sqrt{2}} - \frac{a}{\sqrt{2}} \right)}{t}$$

$$\dot{R} = \frac{1}{2t} \left( a^0 - \sqrt{A\sqrt{2}} \right) \quad \text{in a direction perpendicular to the } \{110\} \text{ planes}$$

$$\dot{R}' = \frac{1}{2t} \left( b^0 - \sqrt{A/\sqrt{2}} \right) \quad \text{in a direction perpendicular to the } \{100\} \text{ planes}$$

Using typical values for all these parameters taken from experimental results, the actual dissolution rates were calculated and compared to

$$\dot{R}^0 = \frac{\text{Vol removed}}{A^0 t}$$

The inherent errors were

< 100 >      ~ 10%

< 111 >      ~ 6%

< 110 >      ?

Since the procedure used for < 110 > above was highly idealized, any calculations based upon this result would be meaningless.

Aeronautical Systems Division, AF Materials Laboratory, Metals and Ceramics Division, Wright-Patterson AFB, Ohio  
Rpt No. ASD-TDR-65-473. ETCH PIT INVESTIGATION OF IRON WHISKERS. Summary report No. 2, Apr 62, 79 p., incl illus., tables, 38 refs. Unclassified Report

The etch pit method applied to small iron single crystals by investigating the shape and position with respect to the crystal axis and the number of dislocations or etch pits in whisker crystals was continued. Dissolution behavior and etch-pit formation were studied in nitric, picric, hydrochloric-cuprous chloride, hydrofluoric-ferric fluoride, copper-ammoniacal chloride and

( over )

sulfuric-potassium persulfate solutions. Geometric pits formed by halide-containing etchants probably results from poisoning of dissolution ledges. A shell (or overgrowth) ranging in thickness from one to several microns was observed frequently and is believed to be a critical factor in the development of distinct etch pits.

Dissolution rates were determined for iron in a solution of  $\text{HF-H}_2\text{O-FeF}_3$  as functions of the crystallographic index of the substrate surface, degree of undersaturation of the dissolving species and the poison concentration.

1. Iron Whiskers
2. Etch-Pit Formation
3. Dissolution Behavior of Etch Pits

- I. AFSC Project 7353, Task 735304
- II. Contract No. AF 33(616)-8252
- III. Ohio State University, Columbus, O.
- IV. Beck, F. H., and Fontana, M. G.
- V. Secondary Rpt No. 1262-2
- VI. In ASTIA collection
- VII. Available fr OTS

Aeronautical Systems Division, AF Materials Laboratory, Metals and Ceramics Division, Wright-Patterson AFB, Ohio  
Rpt No. ASD-TDR-65-473. ETCH PIT INVESTIGATION OF IRON WHISKERS. Summary report No. 2, Apr 62, 79 p., incl illus., tables, 38 refs. Unclassified Report

The etch pit method applied to small iron single crystals by investigating the shape and position with respect to the crystal axis and the number of dislocations or etch pits in whisker crystals was continued. Dissolution behavior and etch-pit formation were studied in nitric, picric, hydrochloric-cuprous chloride, hydrofluoric-ferric fluoride, copper-ammoniacal chloride and

( over )

sulfuric-potassium persulfate solutions. Geometric pits formed by halide-containing etchants probably results from poisoning of dissolution ledges. A shell (or overgrowth) ranging in thickness from one to several microns was observed frequently and is believed to be a critical factor in the development of distinct etch pits.

Dissolution rates were determined for iron in a solution of  $\text{HF-H}_2\text{O-FeF}_3$  as functions of the crystallographic index of the substrate surface, degree of undersaturation of the dissolving species and the poison concentration.

1. Iron Whiskers
  2. Etch-Pit Formation
  3. Dissolution Behavior of Etch Pits
- I. AFSC Project 7353, Task 735304
  - II. Contract No. AF 33(616)-8252
  - III. Ohio State University, Columbus, O.
  - IV. Beck, F. H., and Fontana, M. G.
  - V. Secondary Rpt No. 1262-2
  - VI. In ASTIA collection
  - VII. Available fr OTS